AGU PUBLICATIONS

JGR

Journal of Geophysical Research: Atmospheres

RESEARCH ARTICLE
10.1002/2016JD025321

Special Section:
The Arctic: An AGU Joint Special Collection

# Multidecadal trends in aerosol radiative forcing over the Arctic: Contribution of changes in anthropogenic aerosol to Arctic warming since 1980

**Thomas J. Breider[1], Loretta J. Mickley[1], Daniel J. Jacob[1], Cui Ge[2,3], Jun Wang[2,3], Melissa Payer Sulprizio[1], Betty Croft[4], David A. Ridley[5], Joseph R. McConnell[6], Sangeeta Sharma[7], Liaquat Husain[8], Vincent A. Dutkiewicz[8], Konstantinos Eleftheriadis[9], Henrik Skov[10], and Phillip K. Hopke[11]**

[1]John A. Paulson School of Engineering and Applied Sciences, Harvard University, Cambridge, Massachusetts, USA, [2]Center for Global and Regional Environmental Research, University of Iowa, Iowa City, Iowa, USA, [3]Department of Chemical and Biochemical Engineering, University of Iowa, Iowa City, Iowa, USA, [4]Department of Physics and Atmospheric Science, Dalhousie University, Halifax, Nova Scotia, Canada, [5]Department of Civil and Environmental Engineering, Massachusetts Institute of Technology, Cambridge, Massachusetts, USA, [6]Desert Research Institute, Reno, Nevada, USA, [7]Atmospheric Science and Technology Directorate, Climate Research Division, Environment and Climate Change Canada, Toronto, Ontario, Canada, [8]Atmospheric Sciences Research Center, State University of New York at Albany, Albany, New York, USA, [9]Environmental Radioactivity Laboratory, INRaSTES, NCSR Demokritos, Athens, Greece, [10]Arctic Research Center, Department of Environmental Science, Aarhus University, Roskilde, Denmark, [11]Center for Air Resources Engineering and Science, Clarkson University, Potsdam, New York, USA

**Key Points:**
- Observed sulfate and BC mass concentrations at Arctic surface sites and Greenland ice cores show decreases of 2–3%/yr between 1980 and 2010
- Anthropogenic aerosol RF is negative in the Arctic troposphere due to a large negative RF from sulfate in spring ($-1.17 \pm 0.10$ W m$^{-2}$)
- The 1980–2010 trends in aerosol-radiation interactions over the Arctic and NH midlatitudes contributed $0.27 \pm 0.04$ K warming at Arctic surface

**Correspondence to:**
T. J. Breider,
tbreider@seas.harvard.edu

**Citation:**
Breider, T. J., et al. (2017), Multidecadal trends in aerosol radiative forcing over the Arctic: Contribution of changes in anthropogenic aerosol to Arctic warming since 1980, *J. Geophys. Res. Atmos.*, *122*, doi:10.1002/2016JD025321.

Received 4 MAY 2016
Accepted 9 FEB 2017
Accepted article online 15 FEB 2017



**Abstract** Arctic observations show large decreases in the concentrations of sulfate and black carbon (BC) aerosols since the early 1980s. These near-term climate-forcing pollutants perturb the radiative balance of the atmosphere and may have played an important role in recent Arctic warming. We use the GEOS-Chem global chemical transport model to construct a 3-D representation of Arctic aerosols that is generally consistent with observations and their trends from 1980 to 2010. Observations at Arctic surface sites show significant decreases in sulfate and BC mass concentrations of 2–3% per year. We find that anthropogenic aerosols yield a negative forcing over the Arctic, with an average 2005–2010 Arctic shortwave radiative forcing (RF) of $-0.19 \pm 0.05$ W m$^{-2}$ at the top of atmosphere (TOA). Anthropogenic sulfate in our study yields more strongly negative forcings over the Arctic troposphere in spring ($-1.17 \pm 0.10$ W m$^{-2}$) than previously reported. From 1980 to 2010, TOA negative RF by Arctic aerosol declined, from $-0.67 \pm 0.06$ W m$^{-2}$ to $-0.19 \pm 0.05$ W m$^{-2}$, yielding a net TOA RF of $+0.48 \pm 0.06$ W m$^{-2}$. The net positive RF is due almost entirely to decreases in anthropogenic sulfate loading over the Arctic. We estimate that 1980–2010 trends in aerosol-radiation interactions over the Arctic and Northern Hemisphere midlatitudes have contributed a net warming at the Arctic surface of $+0.27 \pm 0.04$ K, roughly one quarter of the observed warming. Our study does not consider BC emissions from gas flaring nor the regional climate response to aerosol-cloud interactions or BC deposition on snow.

## 1. Introduction

Arctic surface temperatures have increased by ~1.2°C since 1980, while annual average Arctic sea ice coverage has declined by 3.6% per decade [*Trenberth et al.*, 2007; *NSIDC*, 2015]. The factors driving the observed changes in Arctic surface temperatures and sea ice extent are uncertain. Recent studies suggest that accounting for changes in near-term (NT) climate-forcing agents (aerosol, ozone, and methane) might improve global climate model simulations of Arctic warming and sea ice loss [*Mickley et al.*, 2004; *Shindell*, 2007; *Quinn et al.*, 2008; *Yang et al.*, 2014]. Emissions of primary aerosol and aerosol precursors have decreased in recent decades in Europe, Russia, and North America due to air quality concerns, and in situ observations in the Arctic show large declines in concentrations of sulfate and black carbon (BC) aerosol since 1980, consistent with these emission trends [*Gong et al.*, 2010; *Hirdman et al.*, 2010]. In this study we use the GEOS-Chem chemical transport model together with a detailed inventory of historical anthropogenic emissions to quantify decadal changes in Arctic radiative forcing (RF) from trends in aerosols species from 1980 to 2010.

Aerosols perturb the radiative balance of the atmosphere through scattering and absorption of solar radiation, reduction of snow albedo, and alteration of cloud properties [*Twomey*, 1974; *Clarke and Noone*, 1985; *Charlson et al*., 1992]. The radiative impact of Arctic aerosols is modulated by the large seasonal amplitude in available radiation, which peaks in summer [*Quinn et al*., 2008], and in cloud coverage, which peaks in summer to fall [*Shupe et al*., 2011]. Aerosol abundance at remote Arctic stations also shows a distinct seasonal cycle, with a maximum in late winter and early spring known as "Arctic Haze" and a minimum in summer [*Mitchell*, 1956; *Heidam et al*., 2004; *Quinn et al*., 2007]. Aircraft measurements reveal that the aerosol seasonal cycle extends into the Arctic middle to upper troposphere [*Fisher et al*., 2011; *Wang et al*., 2011; *Di Pierro et al*., 2013; *Ancellet et al*., 2014]. The spring peak in aerosol loading arises from efficient pollution transport along isentropic surfaces from the midlatitudes to the Arctic at this time of year [*Rahn and McCaffrey*, 1979; *Radke et al*., 1984; *Shaw*, 1995; *Stohl*, 2006].

Observations of sulfate and BC at remote Arctic stations have shown rapid decreases of 1–3% $yr^{-1}$ since the 1980s [*Sharma et al*., 2004, 2013; *Eleftheriadis et al*., 2009; *Quinn et al*., 2009; *Hirdman et al*., 2010]. Consistent with these trends, ice cores in Greenland and Svalbard Island indicate that sulfate deposition peaked in the 1970s, followed by decline [*Goto-Azuma and Koerner*, 2001; *Isaksson et al*., 2001; *McConnell et al*., 2007]. At Barrow, Alaska, observed background aerosol optical depth (AOD) decreased from 1977 to 2002 but increased slightly between 2002 and 2010 [*Tomasi et al*., 2012]. Many studies have attributed the observed decreases in sulfate and BC in the Arctic to reductions in anthropogenic emissions of primary aerosol and aerosol precursors in Russia and West Eurasia [*Sirois and Barrie*, 1999; *Heidam et al*., 2004; *Gong et al*., 2010; *Hirdman et al*., 2010; *Sharma et al*., 2013]. *Tomasi et al*. [2012] attributed the recent increase in background AOD at Barrow to emissions increases in developing countries at lower latitudes. *Stone et al*. [2014] found an increase of 0.01 per decade in observed background AOD (500 nm) at Barrow, Ny-Alesund, and Alert over the period 2001 to 2012.

Previous studies have used model simulations to investigate how anthropogenic aerosols affect Arctic climate through aerosol effects on radiation, clouds, and surface albedo. *Quinn et al*. [2008] found that anthropogenic aerosol warms the Arctic atmosphere and cools the surface in all seasons, with the largest forcing contribution from BC. *Samset et al*. [2014] estimated the RF from atmospheric BC in the Arctic (70°N–90°N) to be $0.38 \pm 0.30\ W\ m^{-2}$. Previous estimates for the RF from BC in the Arctic atmosphere (60°N–90°N) range from 0.12 to $0.63\ W\ m^{-2}$ [*Koch and Hansen*, 2005; *Flanner et al*., 2009; *AMAP*, 2011; *Bond et al*., 2011; *Wang et al*., 2014a]. Estimates of Arctic RF due to BC deposition to snow and ice range from 0.03 to $0.28\ W\ m^{-2}$ [*Flanner et al*., 2009; *Koch et al*., 2009; *AMAP*, 2011; *Zhou et al*., 2012; *Jiao et al*., 2014]. The Arctic Monitoring and Assessment Programme [*AMAP*, 2015] report, in particular, provided a comprehensive overview of BC RF in the Arctic. The report estimated an average multimodel BC Arctic RF of $0.64\ W\ m^{-2}$.

Several studies have attempted to quantify the contribution of changes in aerosol to Arctic warming in recent decades. *Shindell and Faluvegi* [2009] found that changes in aerosols from 1976 to 2007 contributed $1.09 \pm 0.81$°C to the observed Arctic surface temperature increase of $1.48 \pm 0.28$°C, while *Koch et al*. [2011] found that reductions in BC in the Arctic since 1980 led to cooling at the Arctic surface. In contrast, *Yang et al*. [2014] found no significant response in average Arctic surface temperatures to the 1975–2005 trends in sulfate and BC. *Yang et al*. [2014] did find large regional trends, including a warming in the European Arctic of 0.6 K $decade^{-1}$ and a cooling of 0.6 K $decade^{-1}$ in the Siberian Arctic.

In this paper we use GEOS-Chem to simulate multidecadal trends in distributions of aerosol concentrations in the Arctic. Our aim is first to achieve a satisfactory representation of observed trends in NT climate forcers over decadal timescales in the Arctic and then to quantify the climatic effects of these forcers. Our work builds on the knowledge gained in previous GEOS-Chem studies that focused on the interpretation of measurements during the International Polar Year of 2008 [*Fisher et al*., 2011; *Wang et al*., 2011; *Breider et al*., 2014].

## 2. Model Description

We use the GEOS-Chem chemical transport model version v9-01-03 (http://geos-chem.org) driven by 6-hourly assimilated Modern Era Retrospective Reanalysis (MERRA) meteorology from the NASA Global Modeling and Analysis Office. The original MERRA data are at 0.5° × 0.67° horizontal resolution but are

regridded here to 4° × 5° to enable multidecadal simulations. There are 47 vertical layers extending up to 0.01 hPa.

The GEOS-Chem aerosol simulation includes BC, primary organic carbon (OC), sulfate-nitrate-ammonium, dust, and sea salt and is described in detail by *Breider et al*. [2014].

For primary aerosol, 80% of BC and 50% of OC are emitted in hydrophobic form [*Cooke et al*., 1999]. An *e*-folding time of 1.15 days is assumed for the aging of hydrophobic to hydrophilic aerosol. Oxidation of $SO_2$ to sulfate aerosol takes place via OH in the gas phase and in the aqueous phase by $O_3$ and $H_2O_2$ at temperatures above 258 K [*Alexander et al*., 2009]. Aerosol dry deposition is described in *Fisher et al*. [2011], and the wet deposition scheme is described in *Liu et al*. [2001]. We include updates to aerosol scavenging in convective updrafts and in cold clouds, as described in *Wang et al*. [2014a, 2014b]. The aerosol simulation is coupled to oxidant chemistry through heterogeneous processes, aerosol effects on photolysis rates, formation of secondary aerosol, and inorganic nitrate partitioning. The scheme for dust mobilization accounts for subgrid variability in wind speeds [*Ridley et al*., 2013]. The sea salt aerosol simulation is described by *Jaeglé et al*. [2011], and aerosol optical properties are from *Drury et al*. [2010]. We use the linearized ozone climatological parameterization for stratospheric ozone [*McLinden et al*., 2000].

In their GEOS-Chem analysis of Arctic aerosols, *Breider et al*. [2014] reported an overestimate of Arctic sulfate mass concentrations at the surface in summer. *Croft et al*. [2016] also identified an overestimate of summertime Arctic surface layer accumulation-mode aerosol number concentrations in a version of GEOS-Chem with aerosol microphysics, and these authors pointed to problems in model assumptions of cloud liquid-water content (LWC) in precipitating low-level clouds. The standard GEOS-Chem specifies LWC in such clouds at a globally constant $1.5 \times 10^{-6}$ g m$^{-3}$; spatially and temporally variable fields of LWC have not yet been tested in the model. Observations in summer over the Arctic, however, suggest that LWC in low-level clouds is an order of magnitude lower than the global specified value [*Shupe et al*., 2001]. In our study, we therefore reduce the June–September cloud LWC in GEOS-Chem to a uniform $1 \times 10^{-7}$ g m$^{-3}$ north of 65°N from the surface up to 300 m above the boundary layer, the region of the atmosphere characterized by low-level precipitating clouds in summer. In this manner we effectively increase the aerosol scavenging efficiency in the Arctic and decrease the sulfate concentrations at the Arctic surface in summer by a factor of 2. A more detailed discussion of the sensitivity of cloud scavenging to these model updates is provided by *Croft et al*. [2016].

We use the Fu-Liou radiative transfer model (RTM) to estimate all-sky aerosol RF due to aerosol-radiation interactions over the Arctic [*Wang et al*., 2008, 2013]. The radiative transfer calculation is performed offline using monthly averaged aerosol fields and meteorology from GEOS-Chem. A monthly varying surface reflectance data climatology from the period June 1995 to December 2000 is applied to the RTM [*Koelemeijer et al*., 2003]. The aerosols do not affect cloud properties. The forcing calculation is conducted every 6 h, consistent with input cloud properties. The RTM includes a treatment of cloud fraction overlap, ice crystal effective size, and single scattering properties, and the effect of hygroscopic growth on sulfate particle size and refractive index [*Liou et al*., 2008; *Gu et al*., 2011]. Our calculation provides an estimate of radiative forcing due to aerosol-radiation interactions only (i.e., the direct effect). We do not consider radiative forcing due to aerosol-clouds interactions. We define radiative forcing as the difference in net upwelling radiation between the full aerosol simulation (anthropogenic + natural aerosols) and a simulation with natural aerosols only, often termed the radiative forcing of the aerosol-radiation interactions (ARI) [*Myhre et al*., 2013]. We report the 95th percentile confidence intervals for all forcings.

### 2.1. Historical Emissions

Anthropogenic emissions of primary aerosols (OC and BC) and trace gases—including $NO_x$, CO, $NH_3$, and speciated nonmethane hydrocarbons—are taken from the Monitoring Atmospheric Composition and Climate (MACCcity) inventory for 1980 to 2010 [*Granier et al*., 2011]. MACCcity emissions are based on a simple linear scaling of decadal emissions in the ACCMIP inventory, whose sectors are described in detail in *Lamarque et al*. [2010]. For most species, the simple linear scaling adequately describes the observed trends. Our preliminary simulations showed that the MACCcity $SO_2$ emissions fail to reproduce the steep decline in sulfate concentrations in 1988 observed at Kevo and Ny-Ålesund (Zeppelin), and we therefore update the $SO_2$ emissions inventory following *Smith et al*. [2011]. Compared to MACCcity, *Smith et al*. [2011] provides an improved temporal representation of the emissions drop due to the economic contraction in Eastern Europe after 1988. While retaining the seasonal and spatial information from MACCcity, we apply annual scaling factors to the

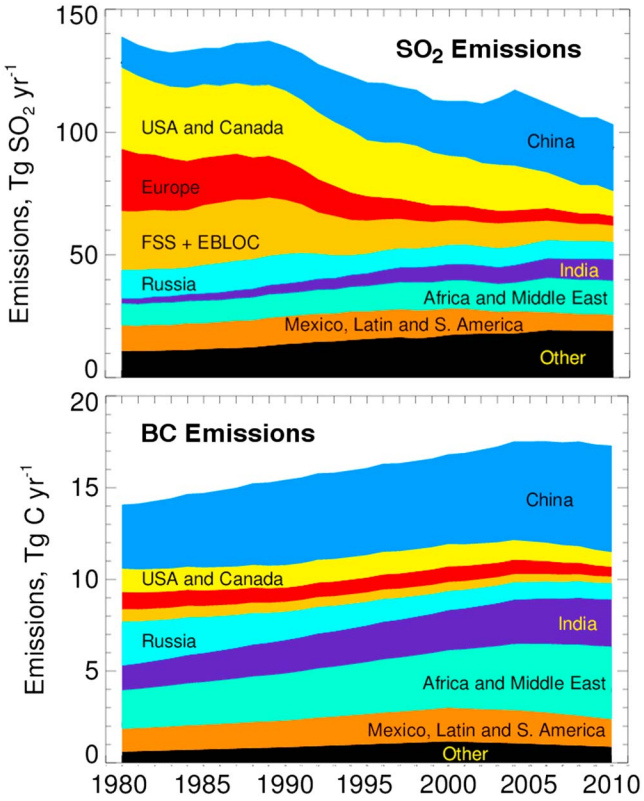


**Figure 1.** Time series of total anthropogenic emissions of (top) $SO_2$ and (bottom) black carbon (BC), classified by region or country. The plot apportions emissions from the former Soviet Union and the Eastern Bloc countries into two categories: (1) Russia and (2) all other former Soviet states (FSS) and eastern bloc countries (excluding East Germany), which we collectively refer to as FSS + EBLOC.

total anthropogenic $SO_2$ emissions across all sectors from every country so that they match the annual national totals from *Smith et al.* [2011]. After 2005, the last year in the *Smith et al.* [2011] inventory, we scale the MACCcity emissions by the mean 2000–2005 ratio of these two inventories for each country.

Emissions estimates of anthropogenic BC vary by a factor of 2 in the present day [*Bond et al.*, 2007; *Cohen and Wang*, 2014], and emissions uncertainties are even larger in previous decades owing to scant information on fuel use and technologies used. We update the MACCcity BC emissions following *Cohen and Wang* [2014]. Again, we retain the seasonal and spatial information from MACCcity but scale the annual emissions in the nine regions specified in *Cohen and Wang* [2014]. Scale factors are calculated as the mean 2002–2006 ratio of annual emissions in the two inventories, the period analyzed by *Cohen and Wang* [2014], and we assume that these factors do not change over time. OC is often coemitted with BC; however, no scaling is applied to anthropogenic OC emissions since our study focuses only on aerosol species with long-term observational records in the Arctic (BC and sulfate). To our knowledge there are no long-term observations of OC in the Arctic that would provide a constraint for an estimate of the multidecadal forcing from OC.

Recent work has shown that gas flaring is an important source of BC in the high Arctic [*Stohl et al.*, 2013; *Eckhardt et al.*, 2015], but given the large uncertainties in this source, we do not include it in our analysis. BC emissions in our study are 126 Gg north of 60°N and 15 Gg north of 66 °N, less than those in *Stohl et al.* [2013], who estimated emissions of 156 Gg and 39 Gg, respectively, with gas flaring emissions included. Our study thus may underestimate BC emissions by 20% north of 60°N and by a factor of 2.6 north of 66°N. The gas flaring source of BC in Russia, however, shows strong temporal variability. *Huang and Fu* [2016] diagnosed a 50% increase in this BC source between 1997 and 2005, followed by a subsequent decline of 40% between 2005 and 2012. BC emissions in Russia in 2010 in our study are 890 Gg, over a factor of 3 higher than the 224 Gg estimated in *Huang et al.* [2015]. The large difference in BC emission estimates between *Huang et al.* [2015] and *Cohen and Wang* [2014] is due to different methodologies (bottom-up versus inverse modeling) and reflects the uncertainties from sparse observations and scant information on the technological emission factors for different BC source estimates.

Figure 1 shows the 1980–2010 time series of $SO_2$ and BC anthropogenic emissions used in this work, aggregated over key regions. We collectively refer to the former Soviet states (excluding Russia) and eastern bloc countries (excluding East Germany) as FSS + EBLOC. Total global emissions of anthropogenic $SO_2$ decrease by 35 Tg $SO_2$ (−20%) between 1980 and 2010. The largest decreases in $SO_2$ emissions during this time take place in Europe (80%) and North America (70%). In FSS + EBLOC and Russia, emissions are almost constant between 1980 and 1988, and subsequently decrease by 50% between 1988 and 2010. Over China, anthropogenic $SO_2$ emissions increase by a factor of 3 between 1980 and 2006, followed by a decline.

**Table 1.** Global and Arctic Budgets of Total and Anthropogenic Aerosols in GEOS-Chem[a]

| Species | Load (mg m$^{-2}$) | | Atmospheric Lifetime (days) | | Total Wet and Dry Deposition (Tg species yr$^{-1}$) | | Fraction Wet Deposition (%) | | Fraction Dry Deposition (%) | |
|---|---|---|---|---|---|---|---|---|---|---|
| | | | | | *Global Total* | | | | | |
| BC | **0.37** | 0.47 | **4.47** | 4.47 | **15.5** | 20.1 | **74** | 77 | **26** | 23 |
| OC | **1.02** | 1.09 | **4.36** | 4.36 | **43.8** | 48.5 | **80** | 82 | **20** | 18 |
| Sulfate | **2.99** | 2.53 | **4.15** | 3.66 | **134** | 129 | **84** | 85 | **16** | 15 |
| | | | | | *Global Anthropogenic* | | | | | |
| BC | **0.33** | 0.40 | **4.42** | 4.29 | **14.0** | 17.5 | **76** | 74 | **24** | 26 |
| OC | **0.26** | 0.29 | **4.32** | 4.23 | **11.1** | 12.8 | **75** | 76 | **25** | 24 |
| Sulfate | **1.71** | 1.49 | **2.84** | 2.62 | **112** | 106 | **87** | 88 | **13** | 12 |
| | | | | | *Arctic Total* | | | | | |
| BC | **0.45** | 0.34 | **7.48** | 7.55 | **0.75** | 0.56 | **78** | 84 | **22** | 16 |
| OC | **0.72** | 1.20 | **5.45** | 5.00 | **1.65** | 3.00 | **81** | 87 | **19** | 13 |
| Sulfate | **5.26** | 3.04 | **6.85** | 7.18 | **9.60** | 5.28 | **87** | 88 | **13** | 12 |
| | | | | | *Arctic Anthropogenic* | | | | | |
| BC | **0.43** | 0.28 | **7.67** | 8.31 | **0.70** | 0.43 | **78** | 83 | **22** | 17 |
| OC | **0.34** | 0.24 | **8.21** | 8.54 | **0.52** | 0.36 | **77** | 80 | **23** | 20 |
| Sulfate | **3.57** | 2.06 | **5.15** | 5.55 | **8.66** | 4.65 | **88** | 90 | **12** | 10 |

[a]Shown are the 1980 (bold) and 2006 annual mean aerosol burdens, atmospheric lifetimes, deposition rates, and fractions of deposition by wet and dry processes, integrated over the troposphere between the surface and 200 hPa. BC and OC values are given in grams carbon. Arctic values are provided for latitudes greater than 60°N.

Global anthropogenic BC emissions in our study increase linearly from 14 Tg C in 1980 to a peak of 17.5 Tg C in 2005 before leveling off. Regionally, BC emissions show much smaller temporal trends than $SO_2$ emissions. BC emissions over Europe and North America decrease by 20% between 1980 and 2010. The smaller decrease in BC emissions relative to sulfate is in part due to increasing numbers of diesel cars and trucks which have higher particulate emissions than gasoline engines [*Bond et al*., 2007]. BC emissions in Russia and FSS + EBLOC decrease by 60% between 1980 and 2010, while BC emissions in China increase by a factor of 2. Historical emissions of $SO_2$ and BC are uncertain in Russia and FSS + EBLOC due to large uncertainties in technology emission factors and few long-term measurements to constrain emissions. In FSS + EBLOC and Russia, the decline in $SO_2$ emissions is reflected by long-term observations of particulate sulfate in these regions. *Sharma et al*. [2004] analyzed Alert BC and back-trajectory data and found that most of the observed decrease in BC at Alert between 1989 and 2002 can be explained by decreases in emissions in the former USSR.

$SO_2$ emissions from erupting and nonerupting volcanoes are from the AeroCom inventory [*Diehl*, 2009]. Oceanic emissions of dimethylsulfide (DMS) are calculated using the DMS seawater climatology from *Lana et al*. [2011] and the sea air gas transfer parameterization from *Liss and Merlivat* [1986].

Constructing a continuous biomass burning inventory for 1980–2010 is challenging. We use biomass burning emissions from *Duncan et al*. [2003] for 1980–1996 and the Global Fire Emissions Database version 3 (GFED3) inventory for 1997–2010 [*van der Werf et al*., 2006]. In most regions, the seasonality of the *Duncan et al*. [2003] inventory is based on area burned data or on retrievals of Aerosol Index from the Total Ozone Mapping Spectrometer. Elsewhere, we apply the 1997–2010 average seasonality from GFED3 to the *Duncan et al*. [2003] inventory. To speciate biomass burning emissions prior to 1997, we use emission factors from *Andreae and Merlet* [2001]. GFED3 misses most small fires [*Randerson et al*., 2012], so we scale these emissions with the mean seasonality measured by the Global Fire Assimilation System [*Kaiser et al*., 2012]. Average 1997–2010 global fire BC emissions in our inventory are 13% higher than during 1980–1996. A previous inventory also estimated higher fire emissions in the 1990s compared to previous decades [*Schultz et al*., 2008]. It is unclear whether this increase reflects the uncertainty inherent in our inventory or whether it arises from an actual increase in recent fire activity at northern latitudes [*Westerling et al*., 2006].

## 3. Observed and Modeled Trends of Arctic Aerosols

We focus our study on changes in sulfate and BC aerosol because long-term observational records are available for these species and both are considered to be important drivers of Arctic climate forcing [*Quinn et al*.,

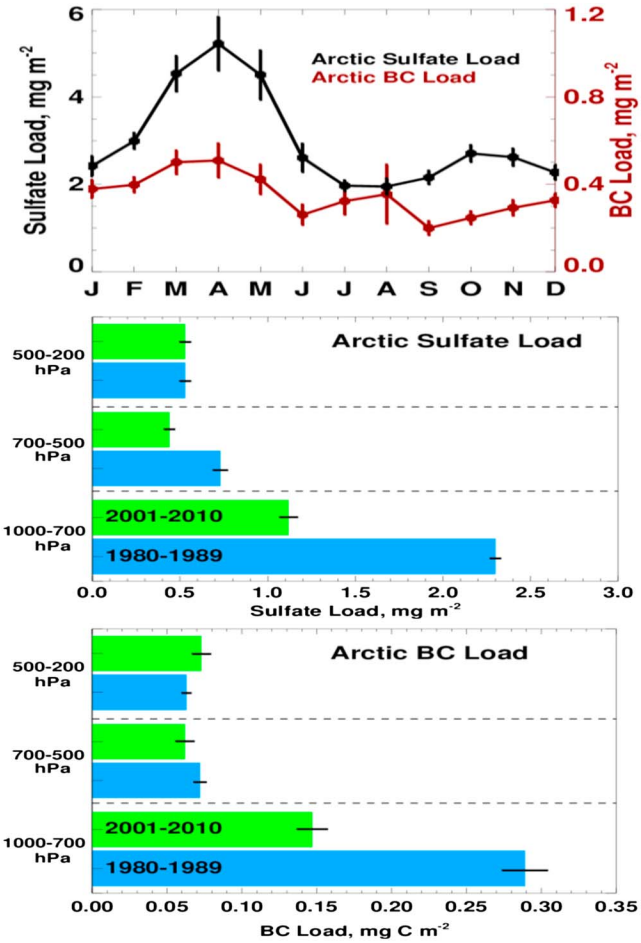


**Figure 2.** (top) Seasonal cycle in the simulated load of sulfate (black) and BC (brown) in the Arctic (>60°N), averaged over the period 2001–2010 in units of mg $m^{-2}$. Vertical bars show 1 standard deviation of the interannual mean. The other two panels compare the simulated mean Arctic loads of (middle) anthropogenic sulfate and (bottom) BC for 1980–1989 versus 2001–2010. Loads are binned by altitude, and the black horizontal bars show 1 standard deviation of the interannual mean in each bin.

2008]. We use arithmetic means throughout our analysis and define the Arctic as the region north of 60°N. To quantify long-term trends in the data, we use the Mann-Kendall Sens Slope estimator of the arithmetic seasonal mass mean concentrations as in *Hirdman et al.* [2010] and *Gong et al.* [2010]. We report only those trends significant at the 95% confidence level. The annual percentage trend is calculated as the overall trend divided by the average of the first five data points in the time series.

### 3.1. Global and Arctic Aerosol Budgets

Table 1 summarizes the global and Arctic aerosol budgets in our simulations for 1980 and 2006. In 2006, the annual mean global loading of anthropogenic sulfate is 1.49 mg $m^{-2}$, down 13% from 1980. The annual mean anthropogenic BC global load is 0.40 mg $m^{-2}$ in 2006, a factor of 3 higher than the average in the Aerosol Comparison between Observations and Models (AeroCom) project phase II simulations [*Myhre et al.*, 2013]. The higher anthropogenic BC load in our study is due to our use of the *Cohen and Wang* [2014] inventory, with BC emissions more than twice those in AeroCom. Using the updated scavenging scheme in convective updrafts [*Wang et al.*, 2014b], we find a global lifetime of atmospheric BC of 4.4 days. Our estimate is at the lower end of AeroCom phase II models, which report a global BC lifetime of 3.9–11.9 days [*Jiao et al.*, 2014]. The short lifetime of BC in our study is explained by relatively more efficient wet scavenging processes and is discussed in *Wang et al.* [2011, 2014b]. Over the Arctic (i.e., north of 60°N), the total sulfate load in our simulations decreases by 42% from 1980 to 2006, even as global $SO_2$ emissions decrease just 3%. The large decrease in the annual mean Arctic sulfate load can be traced to the shift of pollution sources from the high northern latitudes to lower latitudes, from which transport to the Arctic is much less efficient [*Stohl*, 2006]. The modeled annual mean Arctic BC load also decreases by 24% from 1980 to 2010, consistent with declining anthropogenic emissions in the northern midlatitudes.

Figure 2 shows the seasonality of the simulated Arctic load of total BC and sulfate, averaged over the period between 2001 and 2010. The modeled aerosol load is enhanced in spring compared to summer by a factor of 2 for sulfate and by 50% for BC. The figure also presents the simulated annual mean Arctic load of anthropogenic sulfate and BC at three different altitudes, averaged over two time periods, 1980–1989 and 2001–2010. By the 2000s, the annual mean anthropogenic sulfate load decreases by 50% at the surface, 39% in the middle troposphere (700–500 hPa), and 20% in the upper troposphere (500–200 hPa), with the largest changes in spring. The anthropogenic annual mean BC load decreases by 50% at the surface but changes little aloft. The

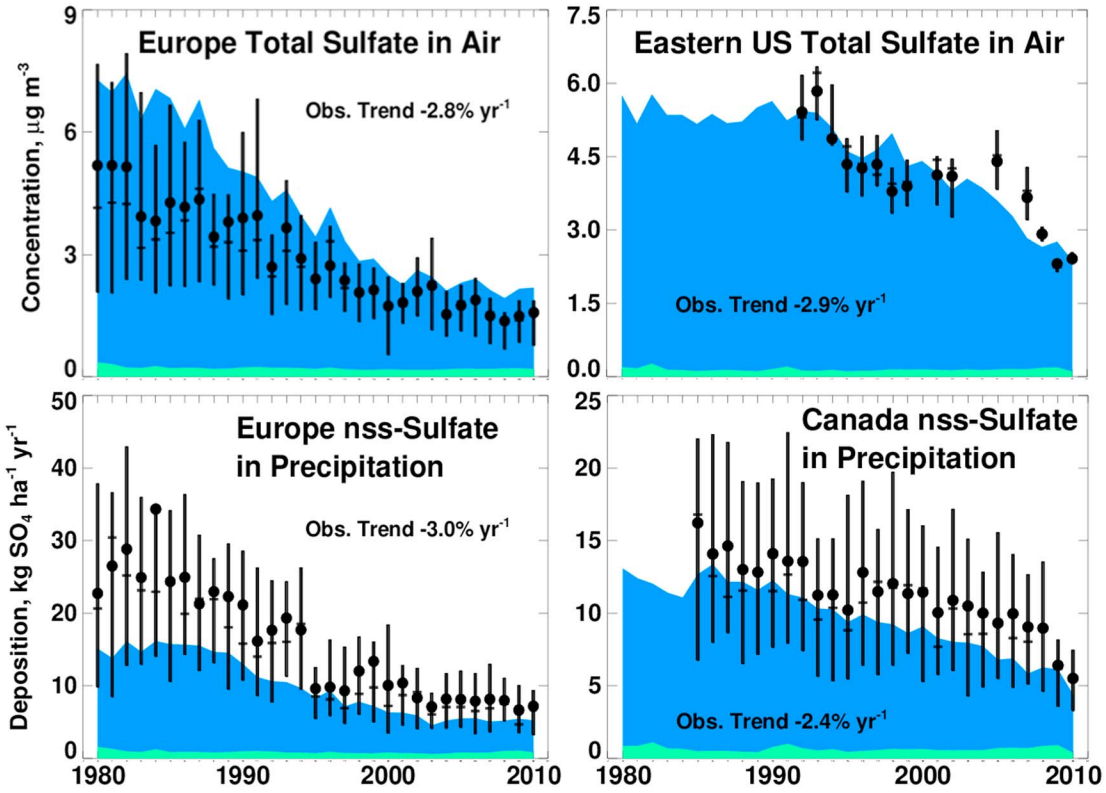


**Figure 3.** Trends in annual mean sulfate concentrations in surface air and in precipitation at sites in Europe and North America. Observations in all panels are shown as black circles, with black bars denoting the standard deviation of the annual means. Stacked contours represent the anthropogenic (blue) and natural (green) contributions to the modeled values. (top left) Trend in total sulfate in surface air, averaged over the 14 EMEP sites with at least 25 years of data between 1980 and 2010. (top right) Trend in total sulfate at the 10 IMPROVE stations on the U.S. East Coast (<90°W) with at least 14 years of data between 1992 and 2010. (bottom left) Trend in nss sulfate in precipitation at the 19 EMEP stations with at least 24 years of data between 1980 and 2010. (bottom right) Trend in nss sulfate in precipitation at the 14 CAPMON stations in Canada with at least 20 years of data between 1984 and 2010.

largest changes in the Arctic BC load occur in winter. This change in the Arctic surface BC load is consistent with the 50% decrease in emissions north of 60°N; however, it is not clear which specific emission sectors are driving the decrease in BC emissions.

### 3.2. Trends in Sulfate Over Source Regions

We next assess the model capability to reproduce observed trends in sulfate over two key source regions, North America and Europe (Figure 3). Over North America we focus our analysis on the eastern part of the U.S. (<90°W), as that region is most relevant for transport of pollution to sites in southern Greenland. Over Europe, the observed 1980–2010 trends in sulfate in surface air ($-2.8\%\ yr^{-1}$) and in precipitation ($-3\%\ yr^{-1}$) are consistent with *Tørseth et al*. [2012]. Over Canada non-sea salt (nss) sulfate deposition shows a decreasing trend of $-2\%\ yr^{-1}$ from 1984 to 2010, while sites in the eastern United States show decreases in sulfate in surface air of $-2.9\%\ yr^{-1}$ from 1992 to 2010. The observed decreases in sulfate in Europe and North

**Table 2.** Observed Trends in Sulfate in Surface Air and in Precipitation in Source Regions[a]

| Sulfate | Europe surface (EMEP[b]) 1980–2010 | | Eastern US surface (IMPROVE[c]) 1992–2010 | | Canada Precip. (CAPMON[d]) 1985–2010 | | Europe Precip. (EMEP[b]) 1980–2010 | |
|---|---|---|---|---|---|---|---|---|
| Annual | **−131.8 (−2.8%)** | −213.8 (−3.0%) | **−155.3 (−3.1%)** | −169.8 (−3.4%) | **−284 (−2.0%)** | −296 (−2.4%) | **−821 (−3.0%)** | −469 (−3.1%) |

[a]Values are absolute trends with units of ng $m^{-3}\ yr^{-1}$ for surface sulfate. Deposition trends in precipitation g $ha^{-1}\ yr^{-1}$ for sulfate. Percentage trends are shown in parentheses (% change $yr^{-1}$). Observed values are shown in bold.
[b]European Monitoring and Evaluation Programme.
[c]Interagency Monitoring of Protected Visual Environments.
[d]Canadian Air and Precipitation Network.

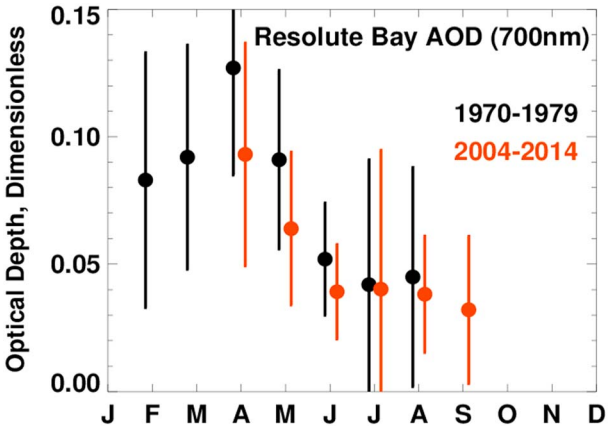


**Figure 4.** Mean seasonality of AOD at 700 nm at Resolute Bay, Canada (75°N, 95°W) for 1970–1979 (black) and 2004–2014 (red). Vertical bars show 1 standard deviation of the mean. Only those monthly averages with at least three data points are shown. Observations for 1970–1979 are from *McGuffie and Cogley* [1985]. Observations for 2004 to 2014 are from AERONET Version 2 data.

America reflect the influence of air quality regulations. Table 2 summarizes the observed and modeled annual trends in sulfate in surface air and in precipitation in Europe and North America. The simulated percentage trends in sulfate and BC are roughly consistent with the observed trends. In Europe, the overestimate in surface sulfate and the underestimate in nss sulfate in precipitation indicate that the aerosol scavenging is too weak in the region.

### 3.3. Trends in Arctic Aerosol Optical Depth

Long-term measurements of AOD help to constrain trends in light extinction by aerosols through the atmosphere column. At Resolute Bay, Canada, observed AOD ($\lambda = 700$ nm) from the 1970s to the present day decreased about $-25$ to $-30$% averaged over April, May, and June (AMJ), yielding a 1975–2010 linear decrease of $-0.8\%\ yr^{-1}$ during these months (Figure 4). Present-day (1997–2010) AOD observations averaged over the eight Arctic sites in the Aerosol Robotic Network (AERONET) reveal the expected springtime maximum, consistent with enhanced transport to the region at this time of year (Figure 5). The annual cycle in Arctic AOD is mainly driven by seasonal changes in the transport and chemical formation of sulfate aerosol. Anthropogenic sulfate contributes over 80% of the total anthropogenic AOD in April and May [*Breider et al.*, 2014]. The large OC component in summer is due to emissions from boreal fires that peak in July and August. Sampled at these eight sites, the model successfully captures the spring peak and September minimum but underestimates AOD by 18% in summer. The summertime bias is largely due to the failure of the model to capture higher Arctic AOD values over Canada at that time of year.

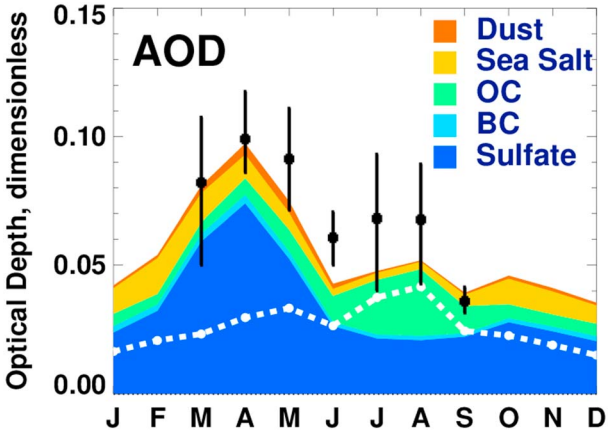


**Figure 5.** Seasonal variation of AOD, averaged over 1997–2010 at eight AERONET stations in the Arctic. The stations used in the figure are Andenes [16.0°E, 69.2°N], Barrow [156.6°W, 71.3°N], Hornsund [15.6°E, 77.0°N], Kangerlussuaq [50.6°W, 70°N], OPAL [85.9°W, 79.9°N], PEARL [86.4°W, 80.0°N], Resolute Bay [94.9°W, 74.7°N], and Thule [68.7°W, 76.5°N]. Black circles denote observed monthly mean AOD, and vertical bars show 1 standard deviation of the means. To remove the influence of large volcanic eruptions in September 2008 and 2009, we exclude these months in the September mean. Monthly means in the plot also do not include outliers, here defined as those months when AOD is greater than $2.7\sigma$ from the mean. This filtering removes 14% of the 234 available observations. Stacked contours represent the contributions from different aerosol types to modeled AOD at 500 nm. White dashed line shows the modeled AOD contribution from natural sources. The model AOD is sampled at 550 nm. The observed AOD at 440 nm is corrected for 550 nm using the Angstrom exponent and assuming a linear fit [*Seinfeld and Pandis*, 2006].

### 3.4. Observed and Modeled Trends in Sulfate and BC at Remote Arctic Surface Stations

Table 3 summarizes the observed seasonal and annual trends in sulfate and BC for the Arctic surface sites and ice cores analyzed in our study. The sites included in our study with long-term observations are Alert (62.5°W, 82.5°N), Barrow (156.6°W, 71.3°N), Ny-Alesund (11.9°E, 78.9°N), Kevo (27.0°E, 69.5°N), and Villum Research Station, Station Nord (VRS) (16.4°W, 81.4°N).

**Table 3.** Observed Trends in Sulfate and Black Carbon at Arctic Sites (North of 60°N), and in Greenland Ice Cores[a]

| Sulfate | Barrow, Alaska 1998–2007 | | Alert, Canada 1981–2010 | | Kevo, Finland 1980–2010 | | Ny-Alesund, Svalbard 1990–2009 | |
|---|---|---|---|---|---|---|---|---|
| Winter | **ns** | ns | **−38.2 (−3.0%)** | −28.3 (−2.4%) | **−46.8 (−2.5%)** | −46.3 (−2.0%) | **−22.7 (−2.7%)** | −34.5 (−2.5%) |
| Spring | **ns** | −17.7 (−1.5%) | **−48.3 (−3.1%)** | −34.8 (−2.7%) | **−84.0 (−2.6%)** | −91.0 (−3.0%) | **ns** | −32.1 (−2.2%) |
| Summer | **+26.8 (+27.9%)** | ns | **ns** | −1.0 (−1.1%) | **−29.5 (−2.1%)** | −40.2 (−3.8%) | **ns** | −9.5 (−3.1%) |
| Fall | **ns** | −12.1 (−2.8%) | **−9.5 (−2.9%)** | −10.5 (−2.3%) | **−33.9 (−2.5%)** | −44.9 (−3.0%) | **−8.2 (−2.4%)** | −16.8 (−2.7%) |
| Annual | **ns** | −10.2 (−1.6%) | **−24.2 (−2.9%)** | −17.0 (−2.3%) | **−45.0 (−2.2%)** | −57.0 (−2.9%) | **−10.7 (−1.7%)** | −24.2 (−2.6%) |
| | **IC[b] Greenland South[c] 1980–2010** | | **IC[b] Greenland Central[d] 1980–2003** | | **IC[b] Greenland North[e] 1980–2010** | | **IC[b] Ackademii Nauk, Russia 1980–1998** | |
| Annual | **−9.5 (−2.2%)** | −15.0 (−1.5%) | **−11.2 (−2.8%)** | −7.8 (−1.3%) | **−5.3 (−2.0%)** | −9.2 (−2.4%) | **ns** | ns |
| **Black carbon** | **Barrow, Alaska 1989–2010** | | **Alert, Canada 1989–2010** | | **Kevo, Finland 1980–2010** | | | |
| Winter | **n/a** | −4.7 (−3.1%) | **−4.7 (−2.9%)** | −6.7 (−3.3%) | **−8.0 (−2.9%)** | −8.3 (−1.8%) | | |
| Spring | **−1.3 (−2.1%)** | −1.5 (−1.9%) | **−2.5 (−2.1%)** | −2.0 (−2.2%) | **−5.3 (−2.1%)** | −7.1 (−2.6%) | | |
| Summer | **ns** | ns | **ns** | −0.1 (−2.8%) | **−2.1 (−2.0%)** | −0.5 (−1.4%) | | |
| Fall | **ns** | −0.8 (−2.7%) | **ns** | ns | **−4.2 (−2.5%)** | −2.6 (−1.7%) | | |
| Annual | **−0.9 (−1.9%)** | −1.4 (−2.0%) | **−1.6 (−2.1%)** | −2.4 (−2.9%) | **−4.5 (−2.2%)** | −4.7 (−2.1%) | | |
| | **IC[b] Greenland South[c] 1980–2010** | | **IC[b] Greenland Central[d] 1980–2003** | | **IC[b] Greenland North[e] 1980–2010** | | **IC[b] Ackademii Nauk, Russia 1980–1998** | |
| Annual | **−0.29 (−2.7%)** | ns | **ns** | +0.43 (+2.6%) | **−0.07 (−1.6%)** | ns | **ns** | ns |

[a]Values are absolute trends with units of ng $m^{-3}$ $yr^{-1}$ for surface sulfate and ng C $m^{-3}$ $yr^{-1}$ for surface BC. Deposition trends in ice cores (IC) are given as g $ha^{-1}$ $yr^{-1}$ for sulfate and g C $ha^{-1}$ $yr^{-1}$ for BC. Percentage trends are shown in brackets (% change $yr^{-1}$). Observed values are shown in bold. Trends that are not significant ($p = 0.05$) are shown as ns.

[b]Ice core observations.

[c]Greenland South includes the ice core stations at Act2 (66.0°N, 45.2°W) and ACT11d (66.5°N, 46.3°W).

[d]Greenland Central includes the ice core station D4 (71.4°N, 43.9°W).

[e]Greenland North includes the ice core stations at Humboldt (78.5°N, 56.8°W), NEEM20m (77.5°N, 51.1°W), Tunu2013 (78.0°N, 34.0°W), and Summit2010 (72.6°N, 38.3°W).

[f]Shown are the 1980 (bold) and 2006 annual mean aerosol burdens, atmospheric lifetimes, deposition rates, and fractions of deposition by wet and dry processes, integrated over the troposphere between the surface and 200 hPa. BC and OC values are given in grams carbon. Arctic values are provided for latitudes greater than 60°N.

Sulfate measurements were made analyzing filter samples using ion-chromatography. The nss sulfate was determined from $Na^+$ concentrations and the mass ratio of sulfate to sodium in seawater of 0.252. Long-term observations of BC have large uncertainties due to changes in instruments over time and interference from other absorbing species such as dust and organic carbon. In this work we use observations of equivalent BC, determined from filter-based absorption measurements using a particle soot absorption photometer or an aethalometer. Absorption measurements are converted to BC mass using an assumed mass absorption coefficient (MAC). MAC values, while well known for freshly emitted BC, are less understood for aged BC and can vary temporally and spatially, thus adding uncertainty [*Sharma et al.*, 2004; *Eleftheriadis et al.*, 2009]. In our study, we use instrument-specific MAC values as discussed in *Stone et al.*, [2014]. Given the large temporal variability in the MAC, estimated BC mass concentrations may have an uncertainty of up to a factor of 2. As a result, the estimated trends in BC mass at Barrow, Alert, and Ny-Alesund are highly uncertain.

Figure 6 shows the observed mean spring (March–May) and summer (June–August) mass concentrations of sulfate aerosol during 1980–2010 at five Arctic sites [*Quinn et al.*, 2007; *Gong et al.*, 2010; *Laing et al.*, 2013; *Nguyen et al.*, 2013]. All stations show higher sulfate concentrations in spring than summer due to more efficient meridional transport, increased surface stratification, and lower rates of removal by precipitation at that time of year [*Stohl*, 2006]. The highest nss sulfate concentrations occur in spring at Kevo in the 1980s, with values about double the concentrations at other Arctic sites, reflecting its closer proximity to pollution sources in western Eurasia than other sites. Between 1980 and 2010, observed sulfate mass in spring decreases by 2–3% $yr^{-1}$ at all sites with the exception of VRS, where observations began only in 1991. Taken together, these trends are consistent with observed trends in sulfate over source regions (Figure 3),

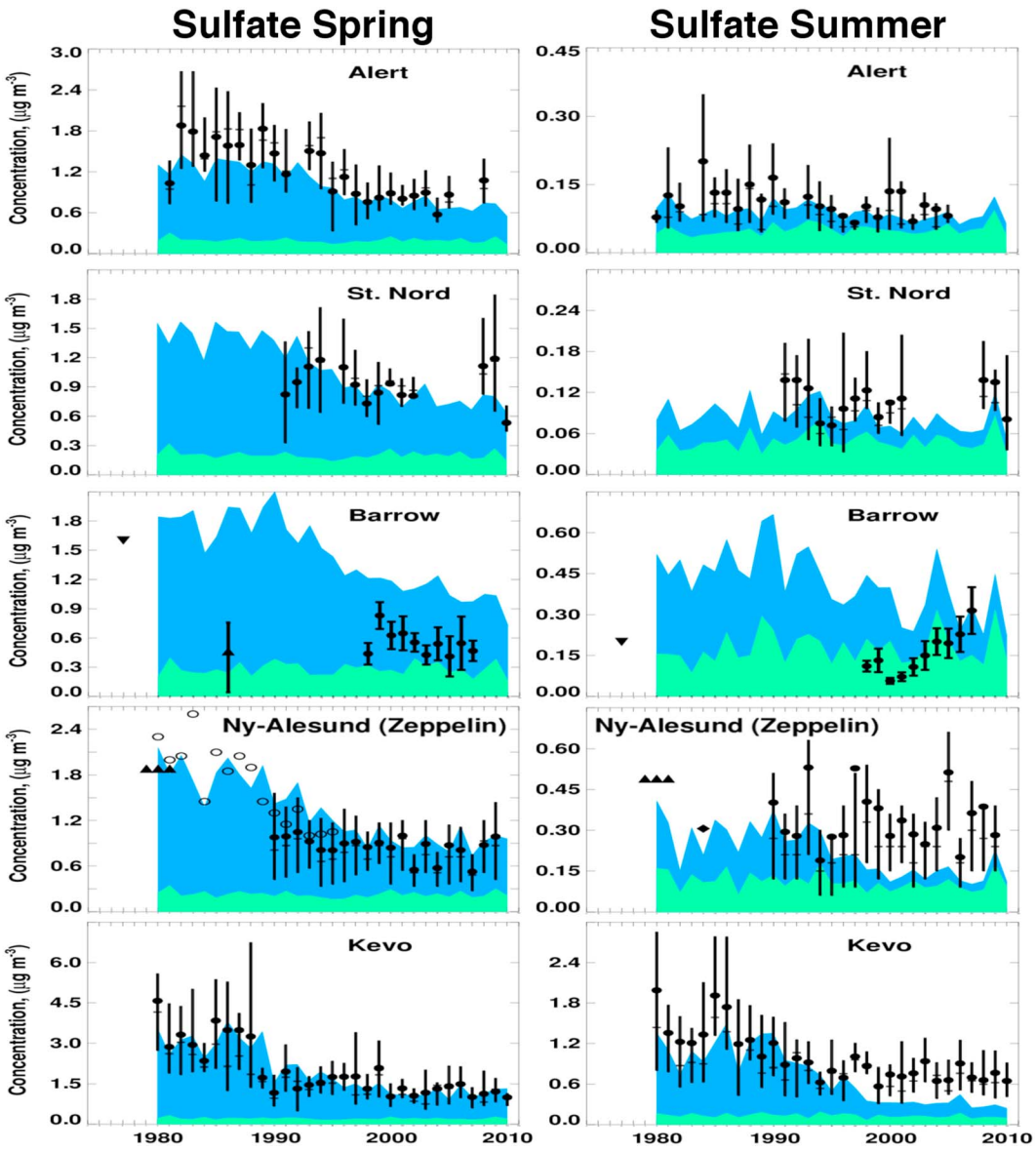


**Figure 6.** Observed nss sulfate surface concentrations at five Arctic sites in spring (March–May) and summer (June–August). Seasonal means are denoted by solid black circles, medians as short horizontal bars, and the 25th to 75th percentile ranges as vertical bars. The observations shown by the solid black circles are provided by the following sources; Alert (Canadian National Atmospheric Chemistry (NAtChem) Database and Analysis System); Villum Research Station, Station Nord, and Ny-Alesund-Zeppelin (European Monitoring and Evaluation Programme (EMEP)); Barrow (NOAA PMEL); and Kevo [*Laing et al*., 2013]). Black triangles early in the record at Barrow are from *Rahn and McCaffrey* [1980] and *Li and Winchester* [1989]. Black triangles at Ny-Ålesund for the period 1979–1981 show mean observations from *Heintzenberg and Larssen* [1983]. Black diamond at Ny-Alesund in summer shows median nss sulfate concentration from *Maenhaut et al*. [1989]. Open circles in the spring panel for Ny-Ålesund are mean March–April values [*Sirois and Barrie*, 1999]. Stacked contours represent the anthropogenic (blue) and natural (green) contributions to the modeled concentrations. Note that the *y* axis range differs among panels.

indicating the influence of more stringent restrictions on air quality. In summer, the more remote Arctic sites (Alert, VRS, and Barrow) show no significant trend in observed surface sulfate mass, which suggests that these sites are not influenced by anthropogenic sources at this time of year.

Observed mean sulfate mass concentrations at Arctic surface sites are overestimated in GEOS-Chem by 4% in spring, while summer mean sulfate is underestimated by 26%. At Barrow the observations are filtered to remove pollution from local sources. We do not remove local pollution sources in our comparison, and this

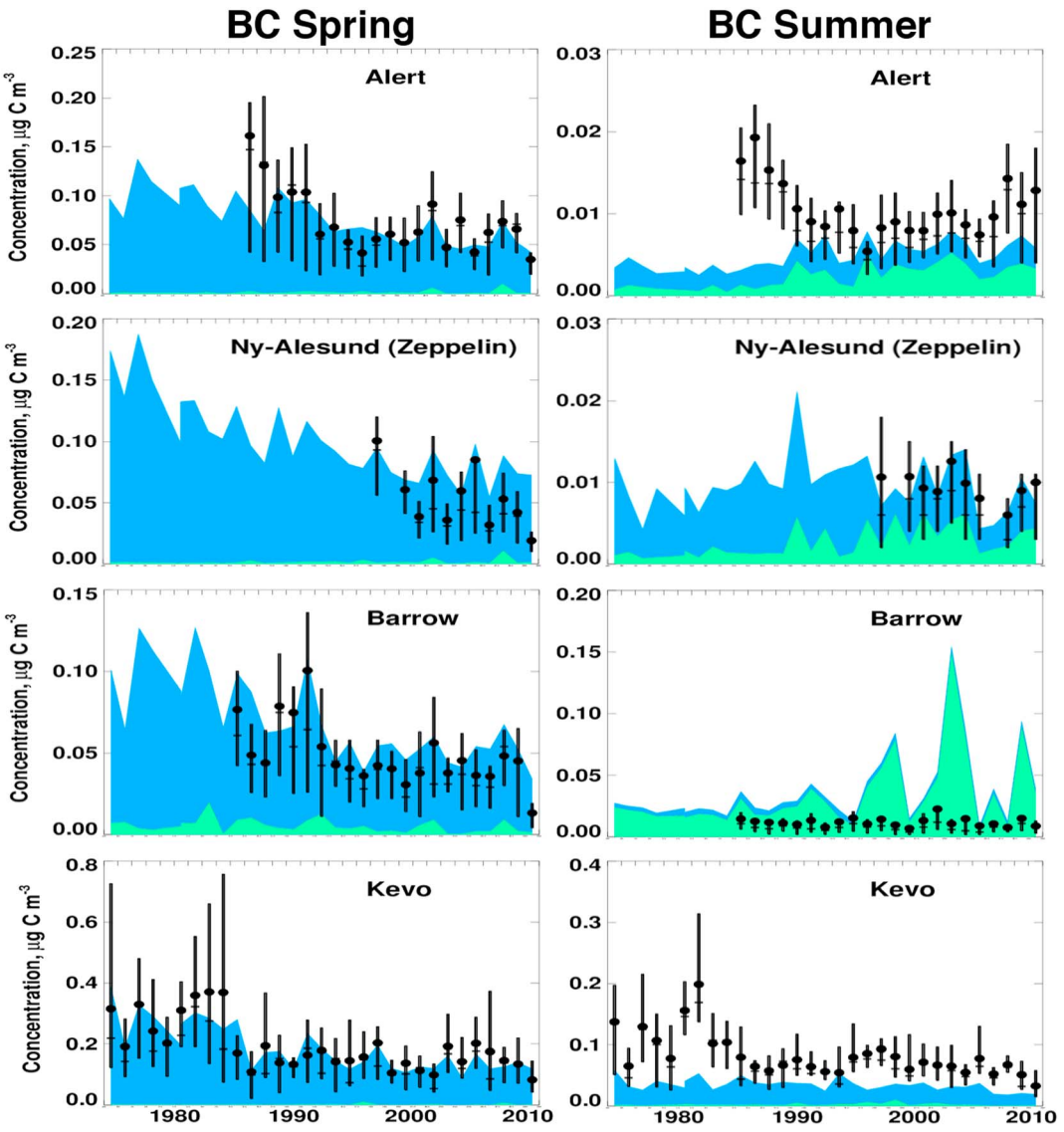


**Figure 7.** Same as Figure 6, but for surface BC at four Arctic sites. The data sources are as follows: *Sharma et al*. [2004, 2006, 2013] at Alert, *Eleftheriadis et al*. [2009] at Ny-Alesund-Zeppelin, NOAA Earth System Research Lab at Barrow, and *Dutkiewicz et al*. [2014] at Kevo.

may explain the model overestimate of annual mean sulfate and sulfate trends at that site. The underestimate at Ny-Alesund may be due to an underestimate in DMS emissions in the North Atlantic. GEOS-Chem reproduces the observed annual mean trends in nss sulfate to within 30% at Kevo and Alert. The large increasing trend in sulfate in summer at Barrow has been reported by *Quinn et al*. [2009]. A similar trend in MSA (not shown) suggests that the observed trend in sulfate has a biogenic source origin and may be in response to climate changes in the Arctic, including sea ice melt and increasing sea surface temperatures. The failure of GEOS-Chem to capture the observed trend may be due to local influences from anthropogenic sources in Barrow, the use of a fixed DMS seawater climatology, or inadequate representation of local sea ice coverage.

At all sites except Kevo, natural sources of sulfate from oceanic emissions of dimethylsulfide (DMS) and volcanoes contribute 28% of the total nss sulfate mass in spring and over 60% in summer during 2001–2010. The natural source contribution at Kevo is smaller, 18% in spring and 40% in summer. Observations of $SO_2$, the major precursor to sulfate aerosol are reproduced to within 35% at VRS in all seasons except the fall, when the simulation overestimates the observations by 77%.

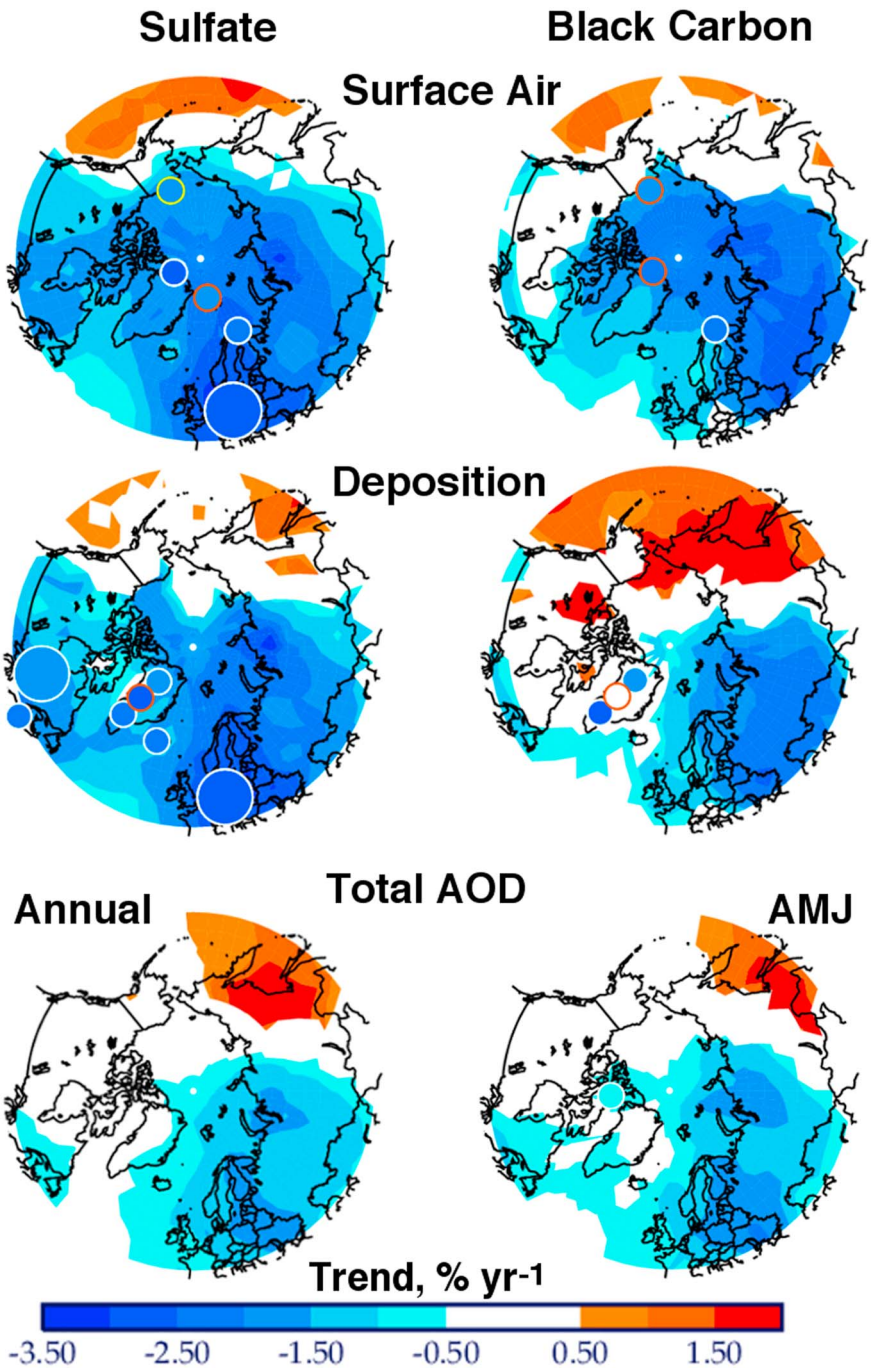


**Figure 8.** Trends in annual mean sulfate and BC concentrations in surface air and in precipitation, as well as in annual mean and April–May–June (AMJ) AOD. Circles indicate observed trends at a range of sites over different time periods: small white circles denote trends at sites with greater than 25 years of observations; large white circles show average long-term trends across multiple sites in Europe and North America; yellow circle, 1976–2002; and red circles 1990–2009. At Ifaross, Iceland, we remove the influence of volcanic sulfate as described in Figure 5. Observed AOD at Resolute Bay, Canada, indicates the mean April–May–June value. GEOS-Chem results are shown as background contours. White indicates regions where the 1980–2010 trend is statistically insignificant or is less than 0.5% $yr^{-1}$.

Tustervatn (65.5°N, 13.5°E) also has long-term (1980–2010) records of both surface sulfate and sulfate in precipitation. As at Kevo, GEOS-Chem captures trends in annual surface sulfate concentrations and sulfate in precipitation at Tustervatn within 30–35%. In Europe, the overestimate in surface sulfate and the

underestimate in nss sulfate in precipitation indicate that the aerosol scavenging is too weak in the region and imply excessive transport of sulfate to the Arctic.

Figure 7 shows the observed mean spring and summer mass concentrations of BC during 1980–2010 at four Arctic sites [*Sharma et al*., 2004, 2013; *Eleftheriadis et al*., 2009; *Dutkiewicz et al*., 2014]. As with sulfate, BC concentrations are higher in spring than summer, when anthropogenic BC from northern midlatitudes is efficiently transported to the Arctic. The observed BC concentrations during spring at the three sites with long-term records (>20 years) show a decreasing trend of between −1.9% $yr^{-1}$ and −2.2% $yr^{-1}$, consistent with the estimated decline in anthropogenic BC emissions in Russia and FSS + EBLOC (−2.1% $yr^{-1}$). In summer, observed trends in BC are weaker or not significant. BC concentrations at Kevo are a factor of 2 higher in spring and a factor of 5 higher in summer relative to other Arctic sites, reflecting the close proximity of this site to pollution sources in western Eurasia. The large drop in BC after 1988 at Kevo has been attributed to the economic contraction in FSS + EBLOC countries at that time [*Dutkiewicz et al*., 2014]. At Kevo, observed trends are underestimated in all seasons except spring, while at Alert, simulated absolute trends are overestimated by 42% in winter (Table 3). Simulated summertime BC at Barrow shows large interannual variability due to the effect of fire activity, an effect not seen in the observations. This mismatch may be explained by the filtering of observations at Barrow, which removes data points when the hourly average wind direction is between 131 and 359°, or due to inaccurate representation of boreal fire emissions between the boundary layer and free troposphere. The updates to the BC emissions and the Arctic summer scavenging processes reduce the disparities between the model and observations. The normalized mean bias improves from−45% to +13% and the $R^2$ value from 0.37 to 0.57.

Ice core records in the Arctic provide a valuable constraint on historical trends in sulfate and BC deposition [*Goto-Azuma and Koerner*, 2001; *McConnell et al*., 2007]. In Figure 8 we compile the observed long-term trends in sulfate and BC in Greenland ice cores and compare these with the observed trends at Arctic surface sites and monitoring stations in Europe and North America. Long-term observations show decreases in annual mean sulfate at all sites of between 2 and 3% $yr^{-1}$. The largest observed surface air trends are found over Europe (−3.0% $yr^{-1}$), and these are consistent with trends in the remote Arctic at Alert (−2.9% $yr^{-1}$). Trends in ice core sulfate in southern Greenland are similar to those observed in surface air in Acadia National Park, USA, and in Ifaross, Iceland, ~2% $yr^{-1}$. Arctic BC observations show decreasing trends of 1.7–2.8% $yr^{-1}$ at all locations, with the exception of the ice core at D4 in central Greenland, where there is no significant trend.

Consistent with these observations, GEOS-Chem shows 1980–2010 decreases of 2–3% $yr^{-1}$ in both surface concentrations and deposition fluxes of sulfate and BC over much of the high northern latitudes and the Arctic (Figure 8). The strongest trends occur over Europe, FSS + EBLOC, and Russia. Simulated concentrations of both sulfate and BC increase by ~1% $yr^{-1}$ over the Pacific due to increasing anthropogenic emissions in East Asia. Simulated AOD also decreases over much of the Arctic, especially in spring, but at much slower rates than the observations, which decrease at about 1% $yr^{-1}$. GEOS-Chem shows a decrease in AMJ AOD at Resolute Bay of −0.6% $yr^{-1}$ for 1980–2010, slightly less than the observed trend of −0.8% $yr^{-1}$ (Figure 5). The model yields no significant trend in BC concentrations over Canada or Alaska, where increasing emissions from boreal fire activity appear to cancel out the effect of decreasing anthropogenic emissions. The lack of a trend in modeled BC over boreal North America stands in contrast to observations of BC in the wider Arctic, which shows decreases over the last three decades. Insufficient knowledge of trends in boreal wildfires in North America may explain the lack of significant trend in the simulated BC deposition in the south of Greenland, where observations show that BC deposition decreased at a rate of 2.7% $yr^{-1}$ between 1980 and 2010. At the high altitudes on top of the Greenland ice sheet, additional uncertainty may arise due to the larger influence of more distant sources at lower latitudes than is typically observed at the Arctic surface stations. Given the many uncertainties in deposition fluxes and the challenge inherent in comparing point measurements with model grid cell averages, our view is that the match between our model and measurements is reasonable.

### 3.5. Observed Aircraft Observations

Aircraft observations have provided sporadic measurements of trace species in the Arctic since the early 1980s. Figure 9 compiles observations of sulfate aerosol over Arctic Canada and Alaska from the Arctic

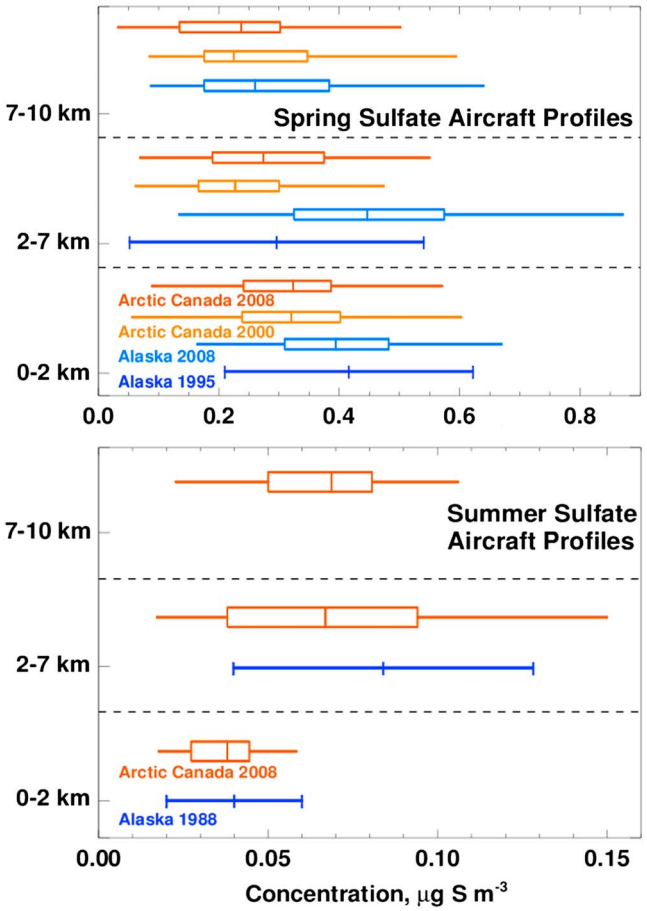


**Figure 9.** Aircraft profile observations of sulfate in the Arctic in spring and summer. Sulfate observations are shown for ARCTAS in 2008 [*Fisher et al.*, 2011], TOPSE in 2000 [*Scheuer et al.*, 2003], Arctic Haze in 1995 [*Jaeschke et al.*, 1999], and ABLE-3A in 1988 [*Talbot et al.*, 1992]. ARCTAS-A sampled in April, and so only TOPSE April flights are used in the comparison. For ARCTAS and TOPSE, we remove outliers that are more than 1.5 interquartile ranges below the first quartile or above the third quartile in each altitude bin. The filtering removes 6% of the 2656 available observations. The box-whisper plots show the minimum, 25th percentile, median, 75th percentile, and maximum values for ARCTAS and TOPSE. The Arctic Haze campaign provides data collected during only three flights from Deadhorse, Alaska, in April [*Jaeschke et al.*, 1999]. For the Arctic Haze and ABLE-3A campaigns, we show only the mean and ±1 standard deviation.

Boundary Layer Expedition [*Talbot et al.*, 1992], the Arctic Haze campaign (1995), the Tropospheric Ozone Production about the Spring Equinox experiment [*Scheuer et al.*, 2003] and the Arctic Research of the Composition of the Troposphere from Aircraft and Satellites campaign [*Jacob et al.*, 2010]. We compare GEOS-Chem with ARCTAS observations by sampling the model along the aircraft flight track. Comparison with earlier campaigns is not possible since some campaigns collected just one or two filter samples per flight.

Below 2 km across all time periods, springtime sulfate concentrations are 20% higher over Alaska than over Arctic Canada, and GEOS-Chem attributes two thirds of this enhancement to a larger influence from natural sources in Alaska. In June–July, aircraft observations of sulfate in the lower troposphere show similar values over Alaska in 1988 and Arctic Canada in 2008, in agreement with surface observations at Alert and VRS.

Model median BC concentrations during ARCTAS are within a factor of 2–3 of observed values. In spring, model median BC concentrations sampled along the aircraft flight tracks north of 70°N are 97 ng $m^{-3}$ below 3 km and 75 ng $m^{-3}$ above 3 km. In summer, model median BC concentrations during ARCTAS flights are 21 ng $m^{-3}$ below 3 km, and 14 ng $m^{-3}$ above 3 km, within a factor of 2 of the observed values. Simulated sulfate concentrations in spring 2008 are captured to within 15% of the observations at all altitudes, while surface sulfate in summer 2008 is overestimated by a factor of 2. Given that column concentrations are more closely associated with RF than surface concentrations, the overestimate in the aircraft BC observations in spring and summer indicates that the BC RF may be overestimated.

### 3.6. Reconciling Observed Trends in Surface and Column Aerosol

Observed sulfate concentrations in surface air in spring show decreases of 2–3% $yr^{-1}$ throughout the Arctic from 1980 to 2010, while AOD decreases by only about 0.5% $yr^{-1}$ (Figure 4). To understand the difference in the observed surface and column trends, we use GEOS-Chem to calculate the contributions of regional changes in anthropogenic emissions to the total change in AOD as a function of altitude for the 1980–2010 time frame for the Arctic as a whole. For each layer of AOD, we aggregate the changes into two regional categories: (1) regions where $SO_2$ emissions have decreased since 1980 (West Eurasia, Russia, and North America) and (2) all other regions including China, where $SO_2$ emissions have increased since 1980.

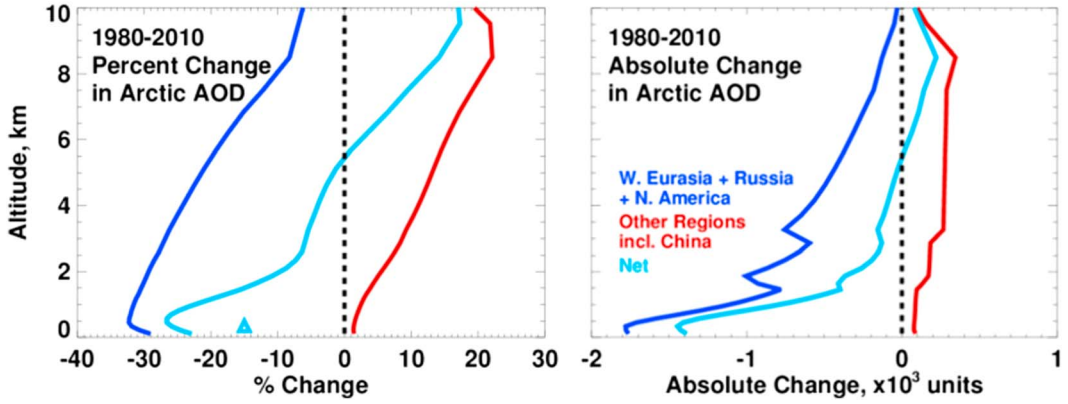


**Figure 10.** Simulated 1980–2010 changes in annual mean layer AOD as a function of altitude, averaged over the Arctic (>60°N). The panels show (left) percent change and (right) absolute change in AOD resulting only from trends in anthropogenic aerosol. The AOD layers correspond to model layers and range in thickness from 125 m at the surface to 1000 m in the upper troposphere. Dark blue curves indicate AOD changes due to sources in West Eurasia, Russia, and North America, and red curves denote changes due to sources in China and elsewhere. Light blue curves represent the net change of AOD in each layer, and the light blue triangle is the simulated percent change in total Arctic AOD.

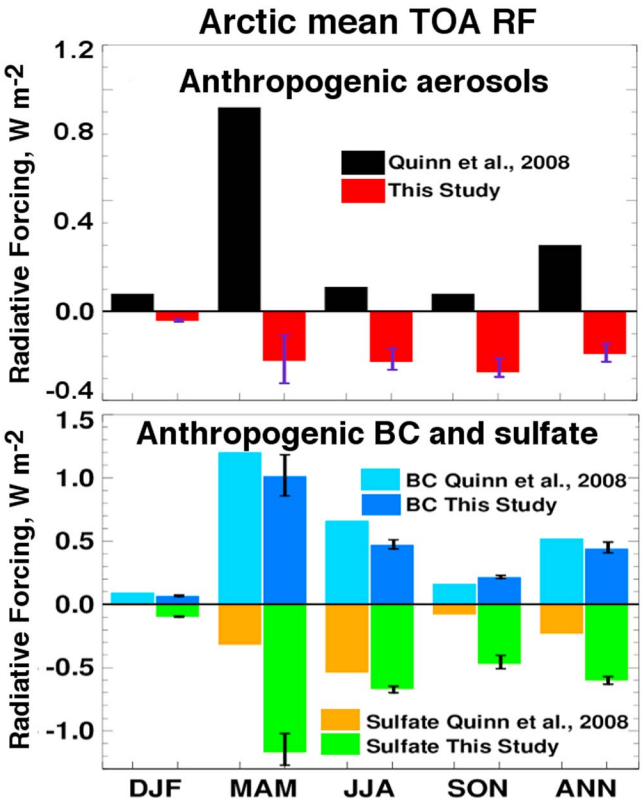


**Figure 11.** Seasonal and annual mean top-of-atmosphere radiative forcings (TOA RFs) due to aerosol, averaged over the Arctic. (top) RFs due to anthropogenic aerosol calculated by this study for 2005–2010 (black) and as reported by *Quinn et al.* [2008] for 2003 (red). (bottom) The sulfate and BC contributions to the RFs in Figure 11 (top) as calculated by this study and by *Quinn et al.* [2008]. Error bars represent ±1 standard deviation of the mean.

We find that the 1980–2010 modeled decrease in total AOD in the Arctic is driven by a combination of strongly decreasing aerosol load at low altitudes and increasing aerosol load at high altitudes (Figure 10). Over the 30 year period, emissions changes in West Eurasia, Russia, and North America yield a ~30% decrease in AOD specific to these regions in the lower troposphere, with less pronounced decreases aloft. In contrast, emissions changes in China and elsewhere yield ~20% increases in region-specific AOD in the upper troposphere, with little effect in the middle to lower troposphere. The altitude dependence of these trends reflect the transport pathways of aerosol from source regions, with the dominant influence from the northern high latitudes at the surface and from lower latitudes aloft [*Stohl*, 2006; *Fisher et al.*, 2010]. The net AOD change in each layer of the troposphere reflects the competition between these two trends, with ~25% decreases in the lower troposphere and ~15% increases in the upper troposphere. The absolute change in total AOD is strongly weighted toward changes in the lower troposphere (Figure 10).

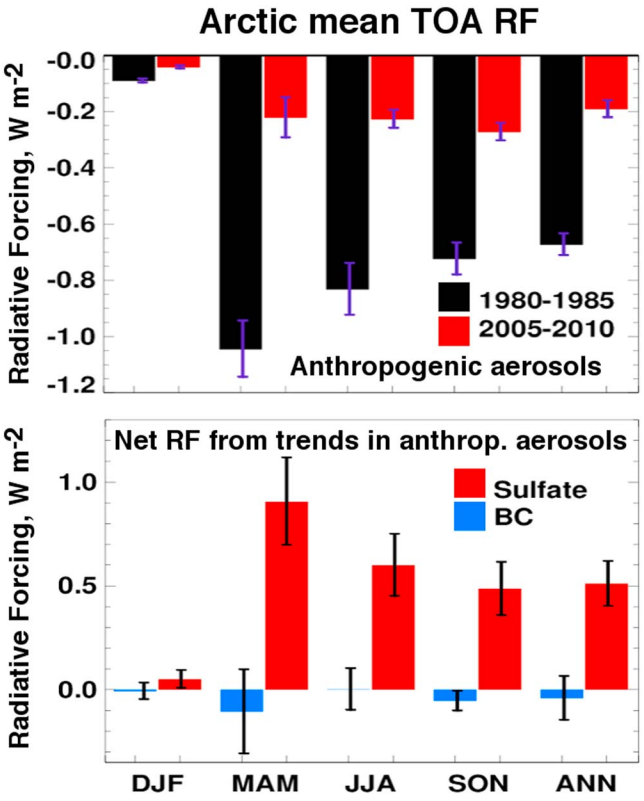


**Figure 12.** Comparison of the seasonal and annual mean TOA RFs due to anthropogenic aerosol during 1980–1985 and 2005–2010, averaged over the Arctic. (bottom) The net RFs due to the trends in sulfate and BC anthropogenic aerosol, calculated as the difference between the mean 2005–2010 and 1980–1985 forcings. Error bars represent ±1 standard deviation of the mean.

## 4. Arctic Aerosol Radiative Forcing Between 1980 and 2010

Applying GEOS-Chem aerosols to the Fu-Liou radiative transfer code, we can estimate for the aerosol RF from aerosol-radiation interactions in the Arctic. We do not consider RF due to BC deposition to snow and ice or due to aerosol-cloud interactions. Our results show that anthropogenic aerosol cools the Arctic troposphere (net negative RF from aerosol). Average 2005–2010 top-of-atmosphere (TOA) RF is $-0.19 \pm 0.05\,\mathrm{W\,m^{-2}}$ (Figure 11), reflecting the balance between negative RF from sulfate ($-0.60 \pm 0.02\,\mathrm{W\,m^{-2}}$) and positive RF from BC ($+0.44 \pm 0.04\,\mathrm{W\,m^{-2}}$). Average TOA forcing from anthropogenic OC is small, $-0.03 \pm 0.003\,\mathrm{W\,m^{-2}}$ and is consistent with results in *Myhre et al.* [2013]. The TOA RF due to OC reflects the small Arctic anthropogenic OC load, which is almost an order of magnitude less than sulfate (Table 1). Surface RF from atmospheric anthropogenic aerosol averaged over the Arctic during 2005–2010 is $-1.20 \pm 0.05\,\mathrm{W\,m^{-2}}$, due to roughly equivalent negative RF from sulfate and BC. Our results stand in contrast to *Quinn et al.* [2008], who found that the interaction of radiation with present-day, anthropogenic aerosol warms the Arctic by $0.92 \pm 0.04\,\mathrm{W\,m^{-2}}$ in spring. The difference between these two results can be traced to the smaller sulfate forcing in *Quinn et al.* [2008], leading to the dominance of BC in total RF. In the model used by *Quinn et al.* [2008], the springtime sulfate burden is enhanced by 40% compared to summer (K. Tsigaridis, personal communication, 2015), while we find a doubling of sulfate at that time of year (Figure 2). The higher Arctic sulfate burden in spring in our work is explained by the lower aerosol scavenging efficiency in cold clouds ($T < 258\,\mathrm{K}$) in GEOS-Chem as described in *Wang et al.* [2011]. ARCTAS aircraft observations in 2008 indicate a factor of 2 enhancement in the Arctic sulfate burden in spring compared to summer. The measurements over Arctic Canada in spring are consistently enhanced by greater than a factor of 2 compared to summer throughout the 25th, 50th, and 75th percentile ranges.

To assess the contribution of aerosol trends to recent Arctic climate change, we examine the net 1980–2010 RF due to anthropogenic aerosol, calculated as the difference between the mean 2005–2010 forcings and mean 1980–1985 forcings. At TOA, we calculate a change in annual mean, net positive Arctic aerosol RF of $+0.48 \pm 0.06\,\mathrm{W\,m^{-2}}$ over this time period (Figure 12), reflecting the trend from strong negative aerosol RF ($-0.67 \pm 0.06\,\mathrm{W\,m^{-2}}$) in the 1980s to more moderate negative aerosol RF in the present day ($-0.19 \pm 0.05\,\mathrm{W\,m^{-2}}$). The 1980–2010 decline in anthropogenic sulfate contributes a net TOA RF of $+0.51 \pm 0.05\,\mathrm{W\,m^{-2}}$, while the net TOA RF due to changes in anthropogenic BC is small ($-0.04 \pm 0.04\,\mathrm{W\,m^{-2}}$). At the surface, the net 1980–2010 Arctic RF from anthropogenic aerosol is even larger, $+0.70 \pm 0.05\,\mathrm{W\,m^{-2}}$. Previous studies have suggested that Arctic climate may respond not just to local forcings but also to remote TOA forcing [*Shindell*, 2007]. For the 1980–2010 period over midlatitudes (28–60°N), we estimate a net TOA forcing $+0.31 \pm 0.04\,\mathrm{W\,m^{-2}}$ due to anthropogenic sulfate and, $+0.14 \pm 0.03\,\mathrm{W\,m^{-2}}$ due to

anthropogenic BC. The net Arctic TOA RF from anthropogenic OC is $+0.01 \pm 0.003\,W\,m^{-2}$ and reflects the small change in anthropogenic OC over the period 1980–2010 (Table 1).

A rough assessment of the contribution of aerosol trends to the observed Arctic warming since 1980 requires knowledge of the climate sensitivity ($\lambda$) in the Arctic to both local and remote TOA forcings. Climate sensitivity provides a measure of the response in surface temperatures (°K) to a given change in TOA RF ($W\,m^{-2}$). Here we follow *Shindell and Faluvegi* [2009], who used a global model to derive climate sensitivities in the Arctic due to aerosol-radiation interactions for different aerosol species. For local forcings, *Shindell and Faluvegi* [2009] estimated sensitivities of $+0.36\,K\,(W\,m^{-2})^{-1}$ for sulfate and $-0.08\,K\,(W\,m^{-2})^{-1}$ for BC. For midlatitude (28–60°N) forcings, they estimated sensitivities of $+0.20\,K\,(W\,m^{-2})^{-1}$ for sulfate and $+0.15\,K\,(W\,m^{-2})^{-1}$ for BC. These sensitivities include aerosol-cloud interactions.

We apply the *Shindell and Faluvegi* [2009] sensitivities to the values reported here for Arctic and midlatitude TOA RF from anthropogenic sulfate and BC. These sensitivities are applied uniformly through the column, and we do not consider any changes in the climate sensitivity with altitude as suggested by *Flanner* [2013]. We estimate that between 1980 and 2010, trends in anthropogenic aerosols contribute $+0.27 \pm 0.04\,K$ warming to average Arctic surface temperatures, or approximately 25% of the observed Arctic warming during this time period. Changes in Arctic RF contribute $+0.19 \pm 0.03\,K$ of this warming, while changes in midlatitude RF provide $+0.08 \pm 0.02\,K$ additional warming. The temperature response due to changes in sulfate is $+0.18 \pm 0.02\,K$ for Arctic sulfate and $+0.06 \pm 0.01\,K$ midlatitude sulfate. For BC, changes in the midlatitudes provide an Arctic temperature response of $+0.02 \pm 0.01\,K$, while changes in BC in the Arctic contribute a warming of $+0.01\,K$.

### 4.1. Increased BC RF Efficiency in the Arctic Between 1980 and 2010

Annual BC TOA RF in the Arctic showed no significant change between the early 1980s and late 2000s ($-0.04 \pm 0.04\,W\,m^{-2}$), while the annual Arctic anthropogenic BC load declined by 33%, from $0.42 \pm 0.02\,mg\,m^{-2}$ to $0.28 \pm 0.04\,mg\,m^{-2}$ over the same period. The larger relative decrease in annual BC load compared to the TOA RF from BC indicates that the BC forcing efficiency increased over this period. We find that Arctic BC forcing efficiency increased from $1.07 \pm 0.05\,W\,m^{-2}\,(mg\,m^{-2})^{-1}$ in the early 1980s to $1.57 \pm 0.09\,W\,m^{-2}\,(mg\,m^{-2})^{-1}$ in the late 2000s.

This increase in Arctic BC forcing efficiency is explained by the shifting influence of regional sources. High-latitude sources, particularly those within the polar dome, are efficiently transported to the Arctic surface in winter and early spring, while lower-latitude sources in Asia influence the Arctic free troposphere in middle to late spring [*Stohl*, 2006]. Declining BC emissions at high latitudes have contributed to a lower BC load at the Arctic surface in winter when incident solar radiation is small, while growing BC emissions in East Asia have contributed to a higher BC load in middle to late spring when there is ample incident solar radiation. This redistribution of BC in the Arctic from winter to spring and from lower to higher altitudes explains the larger BC forcing efficiency per unit mass in the present day compared to 1980.

In Arctic spring, we estimate that the redistribution of BC from lower altitudes in the 1980s to higher altitudes today has increased the BC forcing efficiency by approximately 20%. Our results are consistent with *Samset and Myhre* [2015] who showed that Arctic BC RF efficiency increases strongly with altitude. We find no change in the sulfate Arctic TOA RF efficiency. Formation of sulfate aerosol from high-latitude sources is inefficient in winter, due to limited availability of oxidants [*Gong et al*., 2010].

## 5. Discussion and Conclusions

We have used the chemical transport model GEOS-Chem to construct a 3-D representation of Arctic aerosols that is consistent with observed distributions and 1980–2010 aerosol trends. Our goal was to quantify the potential contribution of trends in anthropogenic aerosols to the rapid Arctic warming ($>1\,K$) observed over this time frame. We focused only on the climate response to aerosol-radiation interactions and used the Fu-Liou radiative transfer model together with published estimates of the sensitivity of surface temperatures to regional aerosol radiative forcings [*Shindell and Faluvegi*, 2009].

We find that most Arctic surface and ice core observations show decreases in sulfate and BC concentrations of 2–3% $yr^{-1}$, consistent with estimated emissions reductions in Eurasia and North America. Observed

springtime (April to June) Arctic AOD at Resolute Bay, Canada, decreases over 1975–2010, but the trend is relatively weak ($-0.8\%$ yr$^{-1}$). The weakness of this trend can be traced to the competing influences of decreasing aerosol load in the lower troposphere, driven by emissions trends at high northern latitudes, and increasing aerosol in the middle to upper troposphere, driven by trends in China and other developing countries at lower latitudes.

Our results show that anthropogenic aerosol yields a negative forcing over the Arctic, with a TOA RF of $-0.19 \pm 0.05$ W m$^{-2}$ in the present day (2005–2010) and even greater forcing ($-0.67 \pm 0.06$ Wm$^{-2}$) in the early 1980s. We find that the 1980–2010 emission reductions in anthropogenic aerosols in the developed world may have contributed $+0.27 \pm 0.04$ K warming to present-day Arctic temperatures at the surface or approximately 25% of the observed Arctic warming. About two thirds of the warming can be attributed to forcing from anthropogenic aerosols over the Arctic, with the rest from forcing over midlatitudes.

Our results differ from those of *Quinn et al*. [2008] and the multimodel average in the *AMAP* [2015] report, in which both reported a net positive forcing due to aerosol-radiation interactions in the present day. The *Quinn et al*. [2008] model, however, yields a relatively small enhancement of sulfate load in spring compared to summer, in contradiction with the strong seasonality inferred from aircraft and AOD observations. Our estimate of ARI RF from Arctic BC of $+0.44 \pm 0.04$ W m$^{-2}$ is within the multimodel range in *AMAP* [2015] of 0.30–0.66 W m$^{-2}$. The present-day Arctic ARI RF from sulfate ($-0.60 \pm 0.02$ W m$^{-2}$) in our study is outside the range of estimates in *AMAP* [2015] of $-0.10$ to $-0.50$ W m$^{-2}$ and greater than the multimodel mean in AEROCOM of less than $-0.40$ W m$^{-2}$ [*Myhre et al*., 2013].

Uncertainties in our estimates of aerosol RF may be traced to model mismatches with observations. For example, modeled Arctic sulfate RF may be overestimated in the Eurasian Arctic due to excessive transport of sulfate from Europe, as suggested by Figure 3. In the high Arctic (>70°N), GEOS-Chem overestimates ARCTAS BC observations by factors of 2–3 (Figure 6), indicating that the positive BC forcing in our study may actually be weaker than our estimate of +0.44 Wm$^{-2}$ for the present day. On the other hand, comparison with site data suggests that we underestimate sulfate and BC net RF over Alert in spring and overestimate these RFs in summer (Table 3). The net RF estimate is also dependent on the capability of the model to reproduce the observed trends. Our study suggests that the sign of the observed trends in Arctic BC and sulfate is consistent with the estimated decreases in emissions in Europe, North America, and Russia. However, we emphasize that BC trends from Russian gas flaring trends have not been included in our study.

BC emissions in our work are double those used in previous work for the present day [e.g., *Wang et al*., 2014a, 2014b]. Scaling down our BC emissions would result in weaker BC TOA RF over the Arctic. A factor of 2 decrease in the BC Arctic RF would result in a stronger negative total aerosol TOA RF, increasing by more than a factor of 2 in the late 2000s, but by just 30% in the early 1980s. Using lower BC emissions would have a small effect on our estimate of the net Arctic warming since 1980 because changes in BC contribute less than 10% of the total net aerosol Arctic warming over this time period.

Our results do not take into consideration RF from aerosol-cloud interactions (indirect effects) or deposition of BC to snow or ice surfaces. As context for our results, we note that *AMAP* [2015] estimated RFs from aerosol-cloud interactions considering both anthropogenic and natural sources of +0.10–0.13 W m$^{-2}$ for BC and $-0.40$–0.75 W m$^{-2}$ for sulfate over the Arctic. In another multimodel study, *Jiao et al*. [2014] reported an RF from BC deposition to Arctic snow and ice of +0.17 W m$^{-2}$.

By using surface reflectance climatology, we have not considered changes in surface albedo. In the Arctic, higher surface albedo in the 1980s due to greater sea ice coverage would reduce sulfate RF but increase BC RF, while lower surface albedo in the late 2000s would have the opposite result, with higher sulfate RF and lower BC RF. Our neglect of climate feedbacks from aerosol in GEOS-Chem may also lead to an overprediction in the estimated total net aerosol warming. *Shindell and Faluvegi* [2009] and *Sand et al*. [2013a, 2013b] found a negative Arctic surface temperature response to BC in the atmosphere column due to a weakening of meridional heat transport. As shown by *Flanner* [2013] and *Sand et al*. [2013a], BC in the lower Arctic atmosphere strongly warms the Arctic surface. Our study shows that most of the change in Arctic BC load since 1980 has taken place in the lower atmosphere (Figure 2), indicating that changes in anthropogenic BC since 1980 may have cooled the Arctic surface, thus offsetting some of the warming due to changes in sulfate.

In their multimodel study, *Shindell and Faluvegi* [2009] reconstructed the influence on Arctic climate of the 1976–2007 trends in both local and midlatitude aerosol loads. They found that aerosols may have warmed the Arctic surface over this time frame by as much as $1.09 \pm 0.81$ K, or about 3 times what we calculate for 1980–2010. Their study, however, inferred zonally averaged, midlatitude aerosol forcings as large as +1 to +5 $Wm^{-2}$ for the 1976–2007 time frame, values that seem inconsistent with observed aerosol trends. Finally, *Yang et al*. [2014] found significant warming over the European Arctic in response to recent aerosol trends, but no significant trend in surface temperatures over the Arctic as a whole. Their study, which focused on the 1975–2005 period, estimated similar declines in sulfate AOD over the Arctic to our study, and unlike our study reported slight increases in Arctic BC AOD during this time frame.

Our study provides a comprehensive analysis of observed long-term trends in Arctic BC and sulfate particulate pollution. We have shown that GEOS-Chem is capable of reproducing observed Arctic aerosol seasonality and trends at surface sites to within 30%. We note that modeling observed sulfate and BC concentrations over broad spatial and temporal scales is challenging. Better representation of observations requires improved understanding of historical emissions and deposition processes.

Our use of a simple, offline method to estimate the temperature response to TOA forcing yields only a rough estimate of the influence of aerosol trends on Arctic surface temperatures. Our approach also focuses only on aerosol-radiation interactions and does not take into account aerosol-cloud interactions, the BC-albedo effect, or changes in greenhouse gases. Within these limitations, our study suggests that air quality measures aimed at reducing particulate pollution have inadvertently accelerated warming of the Arctic over the past 30 years.

**Acknowledgments**
This material is based upon work supported by the National Science Foundation under grant NSF ARC-1049021. The authors wish to acknowledge the contributions of the field scientists and organizations that make the observations and maintain research stations. We thank the Canadian Force services Alert for maintenance of the Alert site, Dan Veber for aerosol instrument maintenance, and Desi Toom for providing inorganic analyses. We wish to thank Eric Scheuer for providing TOPSE aircraft sulfate data. We thank the principal investigators Brent Holben, Victoria E. Cachorro Revill, Michael Gausa, Bruce McArthur, Norm O'Neill, Piotr Sobolewski, Kerstin Stebel, Rick Wagener, and their staff for establishing and maintaining the Arctic AERONET sites used in this investigation. The data used are listed in the references and tables. The measurements at Villum Research Station were financially supported by the Danish Environmental Protection Agency with means from the MIKA/DANCEA funds for Environmental Support to the Arctic Region, which is part of the Danish contribution to "Arctic Monitoring and Assessment Program" (AMAP). The data used in this paper can be accessed at dataverse.harvard.edu using doi:10.7910/DVN/Q1FNUH.

## References

Alexander, B., R. J. Park, D. J. Jacob, and S. Gong (2009), Transition metal-catalyzed oxidation of atmospheric sulfur: Global implications for the sulfur budget, *J. Geophys. Res.*, *114*, D02309, doi:10.1029/2008JD010486.

AMAP (2011), The Impact of Black Carbon on Arctic Climate (2011), By: P.K. Quinn, A. Stohl, A. Arneth,T. Berntsen, J. F. Burkhart, J. Christensen, M. Flanner, K. Kupiainen, H. Lihavainen, M. Shepherd, V. Shevchenko,H. Skov, and V. Vestreng, AMAP Tech. Rep., 4, 72 pp., Arctic Monitoring and Assessment Programme (AMAP), Oslo.

AMAP (2015), AMAP Assessment 2015: Black carbon and ozone as Arctic climate forcers, Arctic Monitoring and Assessment Programme (AMAP), Oslo, Norway, vii + 116 pp.

Ancellet, G., J. Pelon, Y. Blanchard, B. Quennehen, A. Bazureau, K. S. Law, and A. Schwarzenboeck (2014), Transport of aerosol to the Arctic: Analysis of CALIOP and French aircraft data during the spring 2008 POLARCAT campaign, *Atmos. Chem. Phys.*, *14*(16), 8235–8254, doi:10.5194/acp-14-8235-2014.

Andreae, M. O., and P. Merlet (2001), Emission of trace gases and aerosols from biomass burning, *Global Biogeochem. Cycles*, *15*(4), 955–966, doi:10.1029/2000GB001382.

Bond, T. C., E. Bhardwaj, R. Dong, R. Jogani, S. Jung, C. Roden, D. G. Streets, and N. M. Trautmann (2007), Historical emissions of black and organic carbon aerosol from energy-related combustion, 1850–2000, *Global Biogeochem. Cycles*, *21*, GB2018, doi:10.1029/2006GB002840.

Bond, T. C., C. Zarzycki, M. G. Flanner, and D. M. Koch (2011), Quantifying immediate radiative forcing by black carbon and organic matter with the Specific Forcing Pulse, *Atmos. Chem. Phys.*, *11*(4), 1505–1525, doi:10.5194/acp-11-1505-2011.

Breider, T. J., L. J. Mickley, D. J. Jacob, Q. Wang, J. A. Fisher, R. Y.-W. Chang, and B. Alexander (2014), Annual distributions and sources of Arctic aerosol components, aerosol optical depth, and aerosol absorption, *J. Geophys. Res. Atmos.*, *119*, 4107–4124, doi:10.1002/2013JD020996.

Charlson, R. J., S. E. Schwartz, J. M. Hales, R. D. Cess, J. A. Coakley, J. E. Hansen, and D. J. Hofmann (1992), Climate forcing by anthropogenic aerosols, *Science*, *255*(5043), 423–430, doi:10.1126/science.255.5043.423.

Clarke, A. D., and K. J. Noone (1985), Soot in the Arctic snowpack: A cause for perturbations in radiative transfer, *Atmos. Environ.*, *19*(12), 2045–2053, doi:10.1016/0004-6981(85)90113-1.

Cohen, J. B., and C. Wang (2014), Estimating global black carbon emissions using a top-down Kalman Filter approach, *J. Geophys. Res. Atmos.*, *119*, 307–323, doi:10.1002/2013JD019912.

Cooke, W. F., C. Liousse, H. Cachier, and J. Feichter (1999), Construction of a $1° \times 1°$ fossil fuel emission data set for carbonaceous aerosol and implementation and radiative impact in the ECHAM-4 model, *J. Geophys. Res.*, *104*, 22,137–22,162.

Croft, B., R. V. Martin, W. R. Leaitch, P. Tunved, T. J. Breider, S. D. D'Andrea, and J. R. Pierce (2016), Processes controlling the annual cycle of Arctic aerosol number and size distributions, *Atmos. Chem. Phys.*, *16*, 3665–3682, doi:10.5194/acp-16-3665-2016.

Di Pierro, M., L. Jaeglé, E. W. Eloranta, and S. Sharma (2013), Spatial and seasonal distribution of Arctic aerosols observed by the CALIOP satellite instrument (2006–2012), *Atmos. Chem. Phys.*, *13*(14), 7075–7095, doi:10.5194/acp-13-7075-2013.

Diehl, T. (2009), A global inventory of volcanic $SO_2$ emissions for hindcast scenarios. [Available at http://www.lscedods.cea.fr/aerocom/AEROCOM_HC/volc/ (Documents updated in subsequent years after 2009). Last accessed February 2013.]

Drury, E., D. J. Jacob, R. J. D. Spurr, J. Wang, Y. Shinozuka, B. E. Anderson, A. D. Clarke, J. Dibb, C. McNaughton, and R. Weber (2010), Synthesis of satellite (MODIS), aircraft (ICARTT), and surface (IMPROVE, EPA-AQS, AERONET) aerosol observations over eastern North America to improve MODIS aerosol retrievals and constrain surface aerosol concentrations and sources, *J. Geophys. Res.*, *115*, D14204, doi:10.1029/2009JD012629.

Duncan, B. N., R. V. Martin, A. C. Staudt, R. Yevich, and J. A. Logan (2003), Interannual and seasonal variability of biomass burning emissions constrained by satellite observations, *J. Geophys. Res.*, *108*(D2), 4100, doi:10.1029/2002JD002378.

Dutkiewicz, V. A., A. M. DeJulio, T. Ahmed, J. Laing, P. K. Hopke, R. B. Skeie, Y. Viisanen, J. Paatero, and L. Husain (2014), Forty-seven years of weekly atmospheric black carbon measurements in the Finnish Arctic: Decrease in black carbon with declining emissions, *J. Geophys. Res. Atmos.*, *119*, 7667–7683, doi:10.1002/2014JD021790.

Eckhardt, S., et al. (2015), Current model capabilities for simulating black carbon and sulfate concentrations in the Arctic atmosphere: A multi-model evaluation using a comprehensive measurement data set, *Atmos. Chem. Phys.*, *15*(16), 9413–9433, doi:10.5194/acp-15-9413-2015.

Eleftheriadis, K., S. Vratolis, and S. Nyeki (2009), Aerosol black carbon in the European Arctic: Measurements at Zeppelin station, Ny-Ålesund, Svalbard from 1998–2007, *Geophys. Res. Lett.*, *36*, L02809, doi:10.1029/2008GL035741.

Fisher, J. A., et al. (2010), Source attribution and interannual variability of Arctic pollution in spring constrained by aircraft (ARCTAS, ARCPAC) and satellite (AIRS) observations of carbon monoxide, *Atmos. Chem. Phys.*, *10*(3), 977–996, doi:10.5194/acp-10-977-2010.

Fisher, J. A., et al. (2011), Sources, distribution, and acidity of sulfate–ammonium aerosol in the Arctic in winter–spring, *Atmos. Environ.*, *45*(39), 7301–7318, doi:10.1016/j.atmosenv.2011.08.030.

Flanner, M. G. (2013), Arctic climate sensitivity to local black carbon, *J. Geophys. Res. Atmos.*, *118*, 1840–1851, doi:10.1002/jgrd.50176.

Flanner, M. G., C. S. Zender, P. G. Hess, N. M. Mahowald, T. H. Painter, V. Ramanathan, and P. J. Rasch (2009), Springtime warming and reduced snow cover from carbonaceous particles, *Atmos. Chem. Phys.*, *9*(7), 2481–2497, doi:10.5194/acp-9-2481-2009.

Gong, S. L., T. L. Zhao, S. Sharma, D. Toom-Sauntry, D. Lavoué, X. B. Zhang, W. R. Leaitch, and L. A. Barrie (2010), Identification of trends and interannual variability of sulfate and black carbon in the Canadian High Arctic: 1981–2007, *J. Geophys. Res.*, *115*, D07305, doi:10.1029/2009JD012943.

Goto-Azuma, K., and R. M. Koerner (2001), Ice core studies of anthropogenic sulfate and nitrate trends in the Arctic, *J. Geophys. Res.*, *106*(D5), 4959–4969, doi:10.1029/2000JD900635.

Granier, C., et al. (2011), Evolution of anthropogenic and biomass burning emissions of air pollutants at global and regional scales during the 1980–2010 period, *Clim. Change*, *109*(1–2), 163–190, doi:10.1007/s10584-011-0154-1.

Gu, Y., K. N. Liou, S. C. Ou, and R. Fovell (2011), Cirrus cloud simulations using WRF with improved radiation parameterization and increased vertical resolution, *J. Geophys. Res.*, *116*, D06119, doi:10.1029/2010JD014574.

Heidam, N. Z., J. H. Christensen, H. Skov, and P. Wåhlin (2004), Monitoring and modelling of the atmospheric environment in Greenland. A review, *Sci. Total Environ.*, *331*(1–3), 5–28.

Heintzenberg, J., and S. Larssen (1983), $SO_2$ and $SO_4$ = in the Arctic: Interpretation of observations at three Norwegian Arctic-Subarctic stations, *Tellus B*, *35B*(4), 255–265, doi:10.1111/j.1600-0889.1983.tb00028.x.

Hirdman, D., J. F. Burkhart, H. Sodemann, S. Eckhardt, A. Jefferson, P. K. Quinn, S. Sharma, J. Ström, and A. Stohl (2010), Long-term trends of black carbon and sulphate aerosol in the Arctic: Changes in atmospheric transport and source region emissions, *Atmos. Chem. Phys.*, *10*(19), 9351–9368, doi:10.5194/acp-10-9351-2010.

Huang, K., and J. S. Fu (2016), A global gas flaring black carbon emission rate dataset from 1994 to 2012, *Sci. Data*, *3*, 160104, doi:10.1038/sdata.2016.104.

Huang, K., J. S. Fu, V. Y. Prikhodko, J. M. Storey, A. Romanov, E. L. Hodson, J. Cresko, I. Morozova, Y. Ignatieva, and J. Cabaniss (2015), Russian anthropogenic black carbon: Emission reconstruction and Arctic black carbon simulation, *J. Geophys. Res. Atmos.*, *120*, 11,306–11,333, doi:10.1002/2015JD023358.

Isaksson, E., et al. (2001), A new ice-core record from Lomonosovfonna, Svalbard: Viewing the 1920–97 data in relation to present climate and environmental conditions, *J. Glaciol.*, *47*(157), 335–345, doi:10.3189/172756501781832313.

Jacob, D. J., J. H. Crawford, H. Maring, A. D. Clarke, J. E. Dibb, L. K. Emmons, R. A. Ferrare, C. A. Hostetler, P. B. Russell, and H. B. Singh (2010), The Arctic Research of the Composition of the Troposphere from Aircraft and Satellites (ARCTAS) mission: Design, execution, and first results, *Atmos. Chem. Phys.*, *10*(11), 5191–5212.

Jaeglé, L., P. K. Quinn, T. S. Bates, B. Alexander, and J.-T. Lin (2011), Global distribution of sea salt aerosols: New constraints from in situ and remote sensing observations, *Atmos. Chem. Phys.*, *11*(7), 3137–3157, doi:10.5194/acp-11-3137-2011.

Jaeschke, W., T. Salkowski, J. P. Dierssen, J. T. Trümbach, U. Krischke, and A. Günther (1999), Measurements of trace substances in the Arctic troposphere as potential precursors and constituents of Arctic haze, *J. Atmos. Chem.*, *34*(3), 291–319, doi:10.1023/A:1006277230042.

Jiao, C., et al. (2014), An AeroCom assessment of black carbon in Arctic snow and sea ice, *Atmos. Chem. Phys.*, *14*(5), 2399–2417, doi:10.5194/acp-14-2399-2014.

Kaiser, J. W., et al. (2012), Biomass burning emissions estimated with a global fire assimilation system based on observed fire radiative power, *Biogeosciences*, *9*(1), 527–554, doi:10.5194/bg-9-527-2012.

Koch, D., and J. Hansen (2005), Distant origins of Arctic black carbon: A Goddard Institute for Space Studies ModelE experiment, *J. Geophys. Res.*, *110*, D04204, doi:10.1029/2004JD005296.

Koch, D., et al. (2009), Evaluation of black carbon estimations in global aerosol models, *Atmos. Chem. Phys.*, *9*(22), 9001–9026, doi:10.5194/acp-9-9001-2009.

Koch, D., et al. (2011), Coupled aerosol-chemistry–climate twentieth-century transient model investigation: Trends in short-lived species and climate responses, *J. Clim.*, *24*(11), 2693–2714, doi:10.1175/2011JCLI3582.1.

Koelemeijer, R. B. A., J. F. de Haan, and P. Stammes (2003), A database of spectral surface reflectivity in the range 335–772 nm derived from 5.5 years of GOME observations, *J. Geophys. Res.*, *108*(D2), 4070, doi:10.1029/2002JD002429.

Laing, J. R., P. K. Hopke, E. F. Hopke, L. Husain, V. A. Dutkiewicz, J. Paatero, and Y. Viisanen (2013), Long-term trends of biogenic sulfur aerosol and its relationship with sea surface temperature in Arctic Finland, *J. Geophys. Res. Atmos.*, *118*, 1–7, doi:10.1002/2013JD020384.

Lamarque, J.-F., T. C. Bond, V. Eyring, C. Granier, A. Heil, Z. Klimont, D. Lee, C. Liousse, A. Mieville, and B. Owen (2010), Historical (1850–2000) gridded anthropogenic and biomass burning emissions of reactive gases and aerosols: Methodology and application, *Atmos. Chem. Phys.*, *10*(15), 7017–7039.

Lana, A., et al. (2011), An updated climatology of surface dimethlysulfide concentrations and emission fluxes in the global ocean, *Global Biogeochem. Cycles*, *25*, GB1004, doi:10.1029/2010GB003850.

Li, S.-M., and J. W. Winchester (1989), Arctic air chemistry resolution of ionic components of late winter Arctic aerosols, *Atmos. Environ*, *23*(11), 2387–2399, doi:10.1016/0004-6981(89)90251-5.

Liou, K. N., Y. Gu, Q. Yue, and G. McFarguhar (2008), On the correlation between ice water content and ice crystal size and its application to radiative transfer and general circulation models, *Geophys. Res. Lett.*, *35*, L13805, doi:10.1029/2008GL033918.

Liss, P. S., and L. Merlivat (1986), Air-sea gas exchange rates: Introduction and synthesis, in *The Role of Air-Sea Exchange in Geochemical Cycling*, edited by P. Buat-Ménard, pp. 113–127, Springer, Netherlands.

Liu, H., D. J. Jacob, I. Bey, and R. M. Yantosca (2001), Constraints from $^{210}$Pb and $^{7}$Be on wet deposition and transport in a global three-dimensional chemical tracer model driven by assimilated meteorological fields, *J. Geophys. Res.*, *106*, 12,109–12,128, doi:10.1029/2000JD900839.

Maenhaut, W., P. Cornille, J. M. Pacyna, and V. Vitols (1989), Arctic air chemistry trace element composition and origin of the atmospheric aerosol in the Norwegian Arctic, *Atmos. Environ.*, *23*(11), 2551–2569, doi:10.1016/0004-6981(89)90266-7.

McConnell, J. R., R. Edwards, G. L. Kok, M. G. Flanner, C. S. Zender, E. S. Saltzman, J. R. Banta, D. R. Pasteris, M. M. Carter, and J. D. W. Kahl (2007), 20th-century industrial black carbon emissions altered Arctic climate forcing, *Science*, *317*(5843), 1381–1384, doi:10.1126/science.1144856.

McGuffie, K., and J. G. Cogley (1985), Climatological analysis of arctic aerosol quality and optical properties at Resolute, N. W. T, *Atmos. Environ.*, *19*(5), 707–714, doi:10.1016/0004-6981(85)90058-7.

McLinden, C. A., S. C. Olsen, B. Hannegan, O. Wild, M. J. Prather, and J. Sundet (2000), Stratospheric ozone in 3-D models: A simple chemistry and the cross-tropopause flux, *J. Geophys. Res.*, *105*(D11), 14,653–14,665, doi:10.1029/2000JD900124.

Mickley, L. J., D. J. Jacob, B. D. Field, and D. Rind (2004), Climate response to the increase in tropospheric ozone since preindustrial times: A comparison between ozone and equivalent $CO_2$ forcings, *J. Geophys. Res.*, *109*, D05106, doi:10.1029/2003JD003653.

Mitchell, M. (1956), Visual range in the polar regions with particular reference to the Alaskan Arctic, *J. Atmos. Terr. Phys. Spec. Suppl.*, 195–211.

Myhre, G., et al. (2013), Radiative forcing of the direct aerosol effect from AeroCom Phase II simulations, *Atmos. Chem. Phys.*, *13*(4), 1853–1877, doi:10.5194/acp-13-1853-2013.

Nguyen, Q. T., H. Skov, L. L. Sørensen, B. J. Jensen, A. G. Grube, A. Massling, M. Glasius, and J. K. Nøjgaard (2013), Source apportionment of particles at Station Nord, North East Greenland during 2008–2010 using COPREM and PMF analysis, *Atmos. Chem. Phys.*, *13*(1), 35–49, doi:10.5194/acp-13-35-2013.

National Snow and Ice Data Center (NSIDC), (2015), Arctic sea ice extent settles at fourth lowest in the satellite record, National Snow and Ice Data Center. [Available at http://nsidc.org/news/newsroom/PR_2015meltseason (Accessed 3 December 2015).]

Quinn, P. K., G. Shaw, E. Andrews, E. G. Dutton, T. Ruoho-Airola, and S. L. Gong (2007), Arctic haze: Current trends and knowledge gaps, *Tellus B*, *59*(1), 99–114, doi:10.1111/j.1600-0889.2006.00238.x.

Quinn, P. K., et al. (2008), Short-lived pollutants in the Arctic: Their climate impact and possible mitigation strategies, *Atmos. Chem. Phys.*, *8*(6), 1723–1735, doi:10.5194/acp-8-1723-2008.

Quinn, P. K., T. S. Bates, K. Schulz, and G. E. Shaw (2009), Decadal trends in aerosol chemical composition at Barrow, Alaska: 1976–2008, *Atmos. Chem. Phys.*, *9*(22), 8883–8888, doi:10.5194/acp-9-8883-2009.

Radke, L. F., P. V. Hobbs, and I. H. Bailey (1984), Airborne observations of Arctic aerosols. III: Origins and effects of air masses, *Geophys. Res. Lett.*, *11*(5), 401–404, doi:10.1029/GL011i005p00401.

Rahn, K. A., and R. J. McCaffrey (1979), Long-range transport of pollution aerosol to the Arctic: A problem without borders, in *Proceedings WMO Symposium on the Long Range Transport of Pollutants*, vol. 538, pp. 25–35, WMO, Sofia.

Rahn, K. A., and R. J. McCaffrey (1980), On the origin and transport of the winter Arctic aerosol*, *Ann. N. Y. Acad. Sci.*, *338*(1), 486–503, doi:10.1111/j.1749-6632.1980.tb17142.x.

Randerson, J. T., Y. Chen, G. R. van der Werf, B. M. Rogers, and D. C. Morton (2012), Global burned area and biomass burning emissions from small fires, *J. Geophys. Res.*, *117*, G04012, doi:10.1029/2012JG002128.

Ridley, D. A., C. L. Heald, J. R. Pierce, and M. J. Evans (2013), Toward resolution-independent dust emissions in global models: Impacts on the seasonal and spatial distribution of dust, *Geophys. Res. Lett.*, *40*, 2873–2877, doi:10.1002/grl.50409.

Samset, B. H., and G. Myhre (2015), Climate response to externally mixed black carbon as a function of altitude, *J. Geophys. Res. Atmos.*, *120*, 2913–2927, doi:10.1002/2014JD022849.

Samset, B. H., et al. (2014), Modelled black carbon radiative forcing and atmospheric lifetime in AeroCom Phase II constrained by aircraft observations, *Atmos. Chem. Phys.*, *14*, 12,465–12,477, doi:10.5194/acp-14-12465-2014.

Sand, M., T. K. Berntsen, Ø. Seland, and J. E. Kristjánsson (2013a), Arctic surface temperature change to emissions of black carbon within Arctic or midlatitudes, *J. Geophys. Res. Atmos.*, *118*, 7788–7798, doi:10.1002/jgrd.50613.

Sand, M., T. K. Berntsen, J. E. Kay, J. F. Lamarque, Ø. Seland, and A. Kirkevåg (2013b), The Arctic response to remote and local forcing of black carbon, *Atmos. Chem. Phys.*, *13*(1), 211–224, doi:10.5194/acp-13-211-2013.

Scheuer, E., R. W. Talbot, J. E. Dibb, G. K. Seid, L. DeBell, and B. Lefer (2003), Seasonal distributions of fine aerosol sulfate in the North American Arctic basin during TOPSE, *J. Geophys. Res.*, *108*(D4), 8370, doi:10.1029/2001JD001364.

Schultz, M. G., A. Heil, J. J. Hoelzemann, A. Spessa, K. Thonicke, J. G. Goldammer, A. C. Held, J. M. C. Pereira, and M. van het Bolscher (2008), Global wildland fire emissions from 1960 to 2000, *Global Biogeochem. Cycles*, *22*, GB2002, doi:10.1029/2007GB003031.

Seinfeld, J. H., and S. N. Pandis (2006), Atmospheric chemistry and physics: From air pollution to climate change, John Wiley Hoboken, N. J.

Sharma, S., D. Lavoué, H. Cachier, L. A. Barrie, and S. L. Gong (2004), Long-term trends of the black carbon concentrations in the Canadian Arctic, *J. Geophys. Res.*, *109*, D15203, doi:10.1029/2003JD004331.

Sharma, S., E. Andrews, L. A. Barrie, J. A. Ogren, and D. Lavoué (2006), Variations and sources of the equivalent black carbon in the high Arctic revealed by long-term observations at Alert and Barrow: 1989–2003, *J. Geophys. Res.*, *111*, D14208, doi:10.1029/2005JD006581.

Sharma, S., M. Ishizawa, D. Chan, D. Lavoué, E. Andrews, K. Eleftheriadis, and S. Maksyutov (2013), 16-year simulation of Arctic black carbon: Transport, source contribution, and sensitivity analysis on deposition, *J. Geophys. Res. Atmos.*, *118*, 943–964, doi:10.1029/2012JD017774.

Shaw, G. E. (1995), The Arctic haze phenomenon, *Bull. Am. Meteorol. Soc.*, *76*(12), 2403–2413, doi:10.1175/1520-0477(1995)076<2403:TAHP>2.0.CO;2.

Shindell, D. (2007), Local and remote contributions to Arctic warming, *Geophys. Res. Lett.*, *34*, L14704, doi:10.1029/2007GL030221.

Shindell, D., and G. Faluvegi (2009), Climate response to regional radiative forcing during the twentieth century, *Nat. Geosci.*, *2*(4), 294–300, doi:10.1038/ngeo473.

Shupe, M. D., T. Uttal, S. Y. Matrosov, and A. S. Frisch (2001), Cloud water contents and hydrometeor sizes during the FIRE Arctic Clouds Experiment, *J. Geophys. Res.*, *106*(D14), 15,015–15,028, doi:10.1029/2000JD900476.

Shupe, M. D., V. P. Walden, E. Eloranta, T. Uttal, J. R. Campbell, S. M. Starkweather, and M. Shiobara (2011), Clouds at arctic atmospheric observatories. Part I: Occurrence and macrophysical properties, *J. Appl. Meteorol. Climatol.*, *50*(3), 626–644, doi:10.1175/2010JAMC2467.1.

Sirois, A., and L. A. Barrie (1999), Arctic lower tropospheric aerosol trends and composition at Alert, Canada: 1980–1995, *J. Geophys. Res.*, *104*(D9), 11,599–11,618, doi:10.1029/1999JD900077.

Smith, S. J., J. van Aardenne, Z. Klimont, R. J. Andres, A. Volke, and S. Delgado Arias (2011), Anthropogenic sulfur dioxide emissions: 1850–2005, *Atmos. Chem. Phys.*, *11*(3), 1101–1116, doi:10.5194/acp-11-1101-2011.

Stohl, A. (2006), Characteristics of atmospheric transport into the Arctic troposphere, *J. Geophys. Res.*, *111*, D11306, doi:10.1029/2005JD006888.

Stohl, A., Z. Klimont, S. Eckhardt, K. Kupiainen, V. P. Shevchenko, V. M. Kopeikin, and A. N. Novigatsky (2013), Black carbon in the Arctic: The underestimated role of gas flaring and residential combustion emissions, *Atmos. Chem. Phys.*, *13*(17), 8833–8855, doi:10.5194/acp-13-8833-2013.

Stone, R. S., Sharma, S., A. Herber, K. Eleftheriadis, and D. W. Nelson (2014), A characterization of Arctic aerosols on the basis of aerosol optical depth and black carbon measurements. [Available at: http://www.elementascience.org/articles/27.]

Talbot, R. W., A. S. Vijgen, and R. C. Harriss (1992), Soluble species in the Arctic summer troposphere: Acidic gases, aerosols, and precipitation, *J. Geophys. Res.*, *97*(D15), 16,531–16,543, doi:10.1029/91JD00118.

Tomasi, C., et al. (2012), An update on polar aerosol optical properties using POLAR-AOD and other measurements performed during the International Polar Year, *Atmos. Environ.*, *52*, 29–47, doi:10.1016/j.atmosenv.2012.02.055.

Tørseth, K., W. Aas, K. Breivik, A. M. Fjæraa, M. Fiebig, A. G. Hjellbrekke, C. Lund Myhre, S. Solberg, and K. E. Yttri (2012), Introduction to the European Monitoring and Evaluation Programme (EMEP) and observed atmospheric composition change during 1972–2009, *Atmos. Chem. Phys.*, *12*(12), 5447–5481, doi:10.5194/acp-12-5447-2012.

Trenberth, K. E., P. D. Jones, P. Ambenje, R. Bojariu, D. Easterling, A. K. Tank, D. Parker, F. Rahimzadeh, J. A. Renwick, and M. Rusticucci (2007), in *Observations: Surface and Atmospheric Climate Change, Chap. 3 of Climate Change 2007: The Physical Science Basis. Contribution of Working Group I to the Fourth Assessment Report of the Intergovernmental Panel on Climate Change*, edited by S. Solomon et al., pp. 235–336, Cambridge Univ. Press, Cambridge, U. K., and New York.

Twomey, S. (1974), Pollution and the planetary albedo, *Atmos. Environ.*, *8*(12), 1251–1256, doi:10.1016/0004-6981(74)90004-3.

van der Werf, G. R., J. T. Randerson, L. Giglio, G. J. Collatz, P. S. Kasibhatla, and A. F. Arellano Jr. (2006), Interannual variability in global biomass burning emissions from 1997 to 2004, *Atmos. Chem. Phys.*, *6*(11), 3423–3441, doi:10.5194/acp-6-3423-2006.

Wang, H., P. J. Rasch, R. C. Easter, B. Singh, R. Zhang, P.-L. Ma, Y. Qian, S. J. Ghan, and N. Beagley (2014a), Using an explicit emission tagging method in global modeling of source-receptor relationships for black carbon in the Arctic: Variations, sources, and transport pathways, *J. Geophys. Res. Atmos.*, *119*, 12,888–12,909, doi:10.1002/2014JD022297.

Wang, J., D. J. Jacob, and S. T. Martin (2008), Sensitivity of sulfate direct climate forcing to the hysteresis of particle phase transitions, *J. Geophys. Res.*, *113*, D11207, doi:10.1029/2007JD009368.

Wang, J., S. Park, J. Zeng, C. Ge, K. Yang, S. Carn, N. Krotkov, and A. H. Omar (2013), Modeling of 2008 Kasatochi volcanic sulfate direct radiative forcing: Assimilation of OMI $SO_2$ plume height data and comparison with MODIS and CALIOP observations, *Atmos. Chem. Phys.*, *13*(4), 1895–1912, doi:10.5194/acp-13-1895-2013.

Wang, Q., et al. (2011), Sources of carbonaceous aerosols and deposited black carbon in the Arctic in winter-spring: Implications for radiative forcing, *Atmos. Chem. Phys.*, *11*(23), 12,453–12,473, doi:10.5194/acp-11-12453-2011.

Wang, Q., D. J. Jacob, J. R. Spackman, A. E. Perring, J. P. Schwarz, N. Moteki, E. A. Marais, C. Ge, J. Wang, and S. R. H. Barrett (2014b), Global budget and radiative forcing of black carbon aerosol: Constraints from pole-to-pole (HIPPO) observations across the Pacific, *J. Geophys. Res. Atmos.*, *119*, 195–206, doi:10.1002/2013JD020824.

Westerling, A. L., H. G. Hidalgo, D. R. Cayan, and T. W. Swetnam (2006), Warming and earlier spring increase western U.S. forest wildfire activity, *Science*, *313*(5789), 940–943, doi:10.1126/science.1128834.

Yang, Q., C. M. Bitz, and S. J. Doherty (2014), Offsetting effects of aerosols on Arctic and global climate in the late 20th century, *Atmos. Chem. Phys.*, *14*(8), 3969–3975, doi:10.5194/acp-14-3969-2014.

Zhou, C., J. E. Penner, M. G. Flanner, M. M. Bisiaux, R. Edwards, and J. R. McConnell (2012), Transport of black carbon to polar regions: Sensitivity and forcing by black carbon, *Geophys. Res. Lett.*, *39*, L22804, doi:10.1029/2012GL053388.